ÇUKUROVA UNIVERSITY
INSTITUTE OF NATURAL AND APPLIED SCIENCES

MSc THESIS

Himmet ÖZARSLAN

DESIGN AND DEVELOPMENT OF A LIGHT WEIGHT COMPOSITE CHASSIS FOR ELECTRIC VEHICLE APPLICATIONS

DEPARTMENT OF AUTOMOTIVE ENGINEERING

ADANA, 2016

ÇUKUROVA UNIVERSITY
INSTITUTE OF NATURAL AND APPLIED SCIENCES

DESIGN AND DEVELOPMENT OF A LIGHT WEIGHT COMPOSITE CHASSIS FOR ELECTRIC VEHICLE APPLICATIONS

Himmet ÖZARSLAN

MSc THESIS

DEPARTMENT OF AUTOMOTIVE ENGINEERING

We certify that the thesis titled above was reviewed and approved for the award of degree of the Master of Science by the board of jury on 05/01/2016.

....	....	....
Prof. Dr. Hakan YAVUZ SUPERVISOR	Asst. Prof. Dr. Kerimcan ÇELEBİ MEMBER	Asst. Prof. Dr. Göktürk M. ÖZKAN MEMBER

This MSc Thesis is written at the Department of Institute of Natural And Applied Sciences of Çukurova University**.**
Registration Number:

Prof. Dr. Mustafa GÖK
Director
Institute of Natural and Applied Sciences

ABSTRACT

MSc. THESIS

DESIGN AND DEVELOPMENT OF A LIGHT WEIGHT COMPOSITE CHASSIS FOR ELECTRIC VEHICLE APPLICATIONS

Himmet ÖZARSLAN

ÇUKUROVA UNIVERSITY
INSTITUTE OF NATURAL AND APPLIED SCIENCES
DEPARTMENT OF AUTOMOTIVE ENGINEERING

Supervisor : Prof. Dr. Hakan YAVUZ
Year: 2016, Pages: 91
Jury : Prof. Dr. Hakan YAVUZ
: Asst. Prof. Dr. Kerimcan ÇELEBİ
: Asst. Prof. Dr. Göktürk M. ÖZKAN

Today, the vehicle technology is being transformed due to environmental impact of fossil fuel and their uses. Especially studies appear to be directed towards development of lightweight and durable chassis system. In this way, along with achieving fuel economy in existing systems, the need for lightweight chassis for electrically powered vehicles are met.

In recent years, stress analysis studies using the finite element method has made significant contributions to the design engineering. With the help of a computer software, stress and deformation analysis of a system can be achieved with very small margin of errors at very much realistic values.

As a part of the study, some sample carbon fiber-epoxy composite material was manufactured and tested. Considering the test results obtained, a car chassis for two passengers is designed using SolidWorks software. The developed composite and aluminum based chassis have been analyzed on the ANSYS software and the development of the chassis has been completed successfully.

Key Words: CFRP Composite, Chassis, Static Structural Analysis, FEM

ÖZ

YÜKSEK LİSANS TEZİ

ELEKTRİKLİ ARAÇ UYGULAMALARI İÇİN HAFİF KOMPOZİT ŞASE TASARIMI VE GELİŞTİRİLMESİ

Himmet ÖZARSLAN

ÇUKUROVA ÜNİVERSİTESİ
FEN BİLİMLERİ ENSTİTÜSÜ
OTOMOTİV MÜHENDİSLİĞİ ANABİLİM DALI

Danışman : Prof. Dr. Hakan YAVUZ
Yıl: 2016, Sayfa: 91
Jüri : Prof. Dr. Hakan YAVUZ
: Yrd. Doç. Dr. Kerimcan ÇELEBİ
: Yrd. Doç. Dr. Göktürk M. ÖZKAN

Günümüzde araç teknolojisi fosil yakıtlar ve çevresel etkileri sebebi ile değişime uğramaktadır. Özellikle yapılan çalışmaların hafif ve dayanıklı şase sistemlerinin geliştirilmesine yöneldiği görülmektedir. Bu şekilde, var olan sistemlerde yakıt tasarrufu sağlanır iken, özellikle elektrikle çalışan araç sistemlerinde öne çıkan hafif şase ihtiyacının da karşılanması amaçlanmaktadır.

Son yıllarda dünya üzerinde sonlu elemanlar metodu kullanılarak yapılan gerilim analizleri mühendislik dünyasına önemli katkılarda bulunmuştur. Özellikle bilgisayar yazılımları yardımı ile şasi üzerinde oluşan gerilim ve deformasyon değerleri çok küçük hata payları ile, gerçeğe yakın değerleri ile hesaplanabilmektedir

Bu çalışmada, karbon fiber-epoxy kompozit malzeme üretimi ve testleri yapılmıştır. Elde edilen test sonuçları dikkate alınarak, iki kişilik bir otomobil şasesi Solidworks çizim programında 3 boyutlu olarak tasarlanmıştır. Oluşturulan kompozit ve alüminyum malzeme esaslı şase, Ansys paket programında incelenerek analiz edilmiş ve başarı ile şase geliştirilmesi tamamlanmıştır.

Anahtar Kelimeler: CFRP Kompozitler, Şasi, Statik Yapı Analizi,Sonlu Elemanlar Metodu

ACKNOWLEDGEMENTS

First of all, I would like to thank to my supervisor, Prof. Dr. Hakan YAVUZ, for his support and encouragement throughout preparation of this thesis.

I sincerely thank Prof. Dr. Kadir AYDIN and the rest of the Automotive Engineering Department for sharing their knowledge and valuable timely completion for this work.

I wish to thank all staff of Automotive Engineering Department and Mechanical Engineering Department at Çukurova University.

I would like to thank Fatih DARICIK for his technical support me about mechanical tests of composite material used in this thesis.

Last but not least, I would like to thank my parents and my wife.

CONTENTS **PAGE**

LIST OF TABLES **PAGE**

LIST OF FIGURES **PAGE**

LIST OF ABBREVIATIONS AND NOMENCLATURE

FOS	: Factor of Safety
FEA	: Finite Element Analysis
CATIA	: Computer Aided Three-dimensional Interactive Application
FEM	: Finite Element Method
FE	: Finite Element
CFRP	: Carbon Fiber Reinforced Plastics
PP	: Polypropylene
PC	: Polycarbonate
ABS	: Acrylonitrile–butadiene–styrene
GMT	: Glass mat thermoplastic
RTM	: Resin transfer molding
PAN	: Polyacrylonitrile
PPS	: Polyphenylene sulphide thermoplastic
TPO	: Thermoplastic polyolefin
CNC	: Computer Numerical Control
ASTM	: American Society for Testing and Materials
V_f	: Fiber Volume Fraction
E	: Modulus of Elasticity
ν	: Poisson's Ratio
σ	: Strength
S	: Shear strength
G	: Modulus of Elasticity in Shear
F^{ohcu}	: Open hole compressive strength
OHC	: Open hole compressive

1. INTRODUCTION

Mainly, the concerns regarding the increase in fuel prices, the limited resources of fossil fuels, the increase in greenhouse gas emissions (main cause of global warming and resulting climate change) have led to the production and development of more efficient vehicles in the automotive industry. Considering that, in a typical operational condition of an internal combustion engine, most of the fuel (90%) is used to transport the chassis of the vehicle and only 10% is used for transporting the passengers in average. Therefore, reducing the chassis load is one of the research directions for reducing the weight of the vehicle and improving the overall fuel consumption.

Automotive industry seems to focus on lightweight structure in internal combustion (IC), because weight reduction in modern vehicles leads to less fuel consumption and as a result lower exhaust emissions. The increase in fuel prices also plays an importance role in fuel efficient automobiles. Reduction of exhaust gas emissions would surely contribute to reduction of greenhouse effects. Besides, if car can be designed to operate on less fuel with higher fuel efficiency, then the dependency on limited fuel resources will also be reduced.

Advanced materials are essential for boosting the fuel economy of modern automobiles while maintaining safety and also performance. So, it is very much clear that a light weight car consumes less energy to accelerate than a heavier vehicle. Therefore, light weight vehicle chassis design using lightweight materials offers great potential for increasing vehicle efficiency. A 10% reduction in vehicle weight can result in a 6%-8% fuel economy improvement (Carpenter, 2008).

In addition, the typical range of an electric vehicle (EV) is not satisfactory yet. Mainly due to the limitation of energy storage that leads to frequent charging. Vehicle weight reduction is one of the potential issues for increasing battery capacity in electric vehicles, as weight of the vehicle is one of the key factors that limits the range of the vehicle. The weight reduction of the vehicle by using lightweight materials allows better performance and also allows traveling of the longer the distances. While any vehicle can use lightweight materials, they are especially important for electric vehicles.

Because of the above reasons, many attempts have been reported by many researchers to replace the heavy metallic material of the automotive components with lighter materials (Badie, 2011; Kim et. al., 2015). Lightweight materials include magnesium, aluminum, advanced high strength steels, titanium as well as polymer matrix composites reinforced with glass and carbon fibers.

The chassis plays an important role in reducing vehicle weight. Automotive chassis are typically manufactured from various metals, such as composed of steel and steel alloys, aluminum and aluminum alloys, magnesium and magnesium alloys. Despite tremendous advantages of the metal based car chassis, they suffer from some severe limitations:

- Increase in weight of automobile chassis
- surplus fuel consumption because of increasing weight of the chassis
- surplus carbon dioxide emissions because of increasing fuel consumption
- lower performance levels due to increasing weight of automobile chassis

Composite materials have received much attention for automotive structures due to their advantages of lightweight, high specific modulus (E/ρ), high specific strength (σ/ρ), corrosion resistance compared to the conventional metallic materials (Lui et. al., 2013; McAuley, 2003). Specific modulus and strength help specifying the performance under certain loading conditions. Table 1.1 shows comparison of mechanical properties of metallic and composite materials (Savage, 2010).

Table 1.1. Mechanical properties of metallic and composite materials.

Material	Density (g/cm^3)	Tensile Strength, σ (MPa)	Tensile Modulus, E (GPa)	Specific Strength (σ/ρ)	Specific Modulus (E/ρ)
Steel	7,8	1300	200	167	26
Aluminum	2,81	350	73	124	26
Titanium	4	900	108	204	25
Magnesium	1,8	270	45	150	25
E glass	2,1	1100	75	524	21,5
Aramid	1,32	1400	45	1060	57
IM Carbon	1,51	2500	151	1656	100
HM Carbon	1,54	1550	212	1006	138

The concept of composite based car chassis was projected to remove to these problems. The composite materials are lighter in weight than the metals. Because of this reason, they can be preferred for designing chassis in place of metallic materials. Composite materials are increasingly becoming popular for manufacturing car parts in automotive industry. They offer great deal of weight savings. From this aspect, composite materials are more advantageous compared to metallic materials. The following list of advantages provides a clearer view of the picture.

- To decrease carbon dioxide emissions due to its lightweight
- To increase performance of car because of decrease of vehicle weight
- To minimize fuel consumption because of decrease of vehicle weight
- High corrosion resistance
- High thermal resistance
- Good fatigue life
- Good energy absorption
- Damaged structures can be easily repaired
- Improved vibration and damping properties
- Design flexibility

As used in automobiles, composite materials are also used in the aerospace industries, F1 race cars, construction industries, sports equipments, maritime industries, musical instruments and in many other engineering fields. Recently, automobile companies have used significant amounts of composite materials for electric vehicles to reduce body weight and also to extend driving range. These materials are used more and more in various components of vehicles, such as bumper, drive shaft, floor segments, fenders, leaf springs, body panel and seating systems etc. Additionally, composite materials are used in the chassis of vehicles (electric vehicles, hybrid vehicles and internal combustion engine vehicles), as seen in Table 1.2. Megacity electric vehicle body structure made by BMW was developed with carbon fiber reinforced plastics (CFRP). Thus, it an extra 100 kg weight for battery group was obtained (Jacob, 2010). Composite materials are also adopted in sport cars like the Alfa Romeo C4 that has a chassis of 65 kg (Anonymous, 2015k). By using composite materials in the Lexus LFA, a weight savings of 100kg over an aluminum design has been obtained (Anonymous, 2015j).

Table 1.2. Composite materials in the chassis of vehicles

Manufacturer	Picture	Body material	Curb weight	Chassis type	Engine
BMW i3 city car (Anonymous, 2015ı)		CFRP (carbon fiber reinforced plastic)	1195 kg	Carbon-fiber monocoque + aluminum frame	Electric motor
BMW i8 sports car (Anonymous, 2015i)		CFRP (carbon fiber reinforced plastic)	1485 kg	Carbon-fiber monocoque + aluminum frame	Hybrid
Lexus LFA (Anonymous, 2015j)		CFRP (carbon fiber reinforced plastic)	1485 kg	Carbon-fiber monocoque + aluminum frame	Internal Combustion Engine
Alfa-Romeo-4c (Anonymous, 2015k)		CFRP (carbon fiber reinforced plastic)	895 kg	Carbon-fiber monocoque + aluminum frame + steel frame	Internal Combustion Engine

Over the recent years, the use of electric vehicles has considerably increased. As a result, the importance of light weight chassis of electric vehicles has also grown. For these vehicles, various lightweight materials can be used to reduce vehicle weight, without change its strength. In this study, as an answer for the above mentioned necessity for electric vehicles, an electric vehicle chassis designed, developed and analyzed for performance.

2. PRELIMINARY WORK

Patel et al. (2013) designed the model of the chassis in solid works 2009 and analyzed the frame of the chassis named as "eicher 11.10" under static loads. analysis was performed using finite element software Ansys with ten node tetrahedral element to obtain optimal chassis design with factor of safety (FOS) 3 (Patel et al., 2013). Vijaykumar and Patel (2012) modeled "EICHER 11.10" type ladder frame chassis with C-cross section profile. Analysis was done on chassis with different cross section profile using finite element software Ansys workbench.

Swami and Tuljapure (2014) designed ladder frame type chassis with C-cross section profile, modelled this chassis with hexagonal finite element Solid 45 and analyzed the static structural analysis of this model using Ansys R13®. Patel et al. (2013) designed and statically analyzed a truck chassis using the Ansys Workbench to investigate the affect of I-profile dimensions. Some researchers performed to obtain 17% weight reduction by their sensitivity analysis (Patel et al., 2013).

Patel et al. (2014) modeled Tata 2516TC type chassis frame with C-cross section profile using PRO-E software. FEA (Finite Element Analysis) was analyzed on the modeled chassis using the Pro-Mechanica by considering FOS of 5 for design (Patel et al., 2014). Bajwa et al. (2013) analytically and numerically analyzed chassis of Tata Super Ace and found out the critically stressed points where the design can be modified for improving the chassis. Whereupon Godse and Patel (2013) optimized Tata Ace chassis using reinforcements at the critically stressed points.

Francis et al. (2014) designed ladder type chassis frame using CATIA V5 software and analyzed this chassis using Ansys R14 with tetrahedral element, by loading with static forces, by considering FOS of 3 for design. Patil et al. (2013a) designed a ladder type low loader truck chassis structure consisting of C-beams and performed stress analysis of the chassis by using FEM to reduce the expenses of the truck chassis by achieving a reduction in the magnitude of stress at critical point of the chassis frame, side member thickness, cross member thickness. The authors concluded that it is better to change the thickness of cross member at critical stress point than changing the thickness of side member and position of chassis for reduction in stress values and deflection of chassis (Patil et al., 2013a). A similar study was performed by Patil and Kachave (2013) to investigate effect of web and flange's thickness on bending stiffness of a ladder type low loader truck chassis structure consisting of C-beams. Nor et al. (2012) modeled, simulated and performed the stress analysis of an actual low loader structure and so exposed the discrepancy between the theoretical (2-D) and numerical (3-D FEA) results.

Kumar et al. (2014) modeled the tubular space frame chassis using Solid Works software and analyzed the static structural test using the Ansys Workbench under the different constraints. It was compared the torsional rigidity of chassis obtained from experimental to the value obtained from the Ansys Workbench software. Mat and Ghani (2012) designed a steel space frame chassis with different cross sectioned profiles by considering lightweight, fuel efficiency, environmentalism.

Croccolo et al. (2011) examined the structural response of an articulated urban bus chassis, with the help of the Finite Elements Method, in terms of stress, strain and displacement, under several loading and constraining conditions, which aim at reflecting the actual duty cycle of the bus.

Lavanya et al. (2014) analyzed a car chassis frame at four types load conditions (Longitudinal Torsion, Vertical Bending, Lateral Bending, Acceleration Test) to compare deflection, bending moment, von mises stress, factor of safety of the chassis.

Singh (2010) analytically calculated static and dynamic load distributions under various boundary conditions and analyzed stress distributions, lateral displacements during static, dynamic and frequency modes to ensure considerably high FOS as required. The author concluded that torsional rigidity was calculated to be 615.98 Nm/deg which was 2.46 times the torsional rigidity of older design (250 Nm/deg) without increasing weight and weight of chassis observed to decrease by 11.11% with approximate value of 32 kg as compared to weight of older chassis frame.

Solghar and Arsalanloo (2013) studied to evaluate the static and dynamic characteristic of Hyundai Cruz minibus by using Abaqus software tool for designing as well as FEA.

Agrawal and Razik (2013) analyzed static and dynamic characteristic for weight reduction of the TATA 1612 chassis. The authors carried out a sensivity analysis to achieve 8,49% weight reduction.

Akbaş et al. (2006) investigated fatigue and static analysis of Otokar's 3-axle semi trailer chassis by means of experimentally and numerically studies and it was shown that experimental and numerical results are consistent. The authors concluded that the thickness of the chassis except weld points could be reduced considering stress distributions.

It was shown by above literature survey that so many static and dynamic analysis were performed with the help of FEM based simulation programs to decrease weight of the chassis and to save natural resources. Because of that the chassis is one of the heaviest components of a vehicle, hence lightweight chassis designs are inevitable. Thus longer travel distance, increased fuel efficiency, low emissions can be obtained and more environmental vehicles with better driving performance can be manufactured. Vehicle manufacturers are also trying to develop many automotive parts using lighter materials to achieve the above goals. For environmental regulations, such as the air pollution from exhaust gas emissions, global climate change from greenhouse gas emissions and saving natural resources, it has become especially important to develop lightweight vehicles, which have high efficiency and low fuel consumption. Because of this, there has been widespread research on development of the lighter materials in place of conventional materials and it has been mostly alternated by laminated composite materials. A summary of studies about design of lightweight of chassis are presented below.

Park et al. (2013) investigated the structural performance of the carbon fiber/epoxy composite ladder frame in place of the original steel ladder frame using the finite element (FE) model of a 2007 Chevrolet Silverado to evaluate characteristics of stiffness tests and frontal impact tests. The results shown that carbon fiber chassis is 32% lighter than the steel frame and 3.2% weight reduction can be achieved on overall vehicle weight.

Liu et al. (2013) applied to crashworthiness analysis of electric vehicle body structure under the roof crash and side pole impact using a multi-scale approach. The three-dimensional material properties predicted by using the finite element based homogenization method were validated by comparing with the uniaxial tensile and three point bending tests. It is shown that the carbon fiber/epoxy composite body structure given rise to 28% saving in the weight compared with the weight of the glass fiber/epoxy composite body structure (Liu et al., 2013).

Feraboli and Masini (2004) presented that bumpers, fenders, hood, etc. is produced from the carbon fiber/epoxy composite having lower density, higher specific strength and superior impact resistance and they offered that use of carbon fiber/epoxy composites for this application ensuring a weight reduction of 34 kg than its predecessor.

Megacity electric vehicle was developed with carbon fibre reinforced plastics (CFRP) vehicle body construction by BMW, to obtain 100 kg body weight reduction and thus extra 100 kg battery group could be added (Jacob, 2010).

Feraboli et al. (2007) designed and manufactured a composite tubular space frame construction on engine of Lamborghini Murcielago Roadster to compensate the losses in torsional and bending stiffness of the roofless vehicle. This composite tubular space frame was 60% lighter and costs within twice of the metallic benchmark.

Vaidya et al. (2004) designed and manufactured glass/PP composite panel for the floor segment of a mass transit bus. This composite floor panel was 40% lighter than the conventional metal/plywood design.

Jeon et al. (2011) investigated PC/ABS based composite substitutes for conventional steels used in a car audio chassis assessed through weight reduction analysis and cost-benefit analysis. The results show that PC/ABS composite audio chassis supplies 51% weight reduction than that of metal one, with same cost.

Li et al. (2004) numerically performed crashworthiness and strength analysis of glass mat thermoplastic (GMT) car body and deduced that there is no considerable difference between mild steel and GMT car body since GMT reduces the body weight by 41 kg.

Cramer and Taggart (2002) studied the design and production method of the composite body for Hypercar Inc.’s Revolution concept vehicle. The design of the passenger safety cell was manufactured by using a resin transfer molding (RTM) with predominantly intermediate modulus PAN based carbon fiber and low-viscosity "Nylon 12 Laurolactam" thermoplastic. The Revolution’s composite body structure (187 kg) is 57% lighter than a conventional steel body structure (430 kg) of the same size. Its composite chassis weight (201.2 kg) was 34% lighter than a conventional steel chassis (306 kg).

Bartus et al. (2006) designed and fabricated E-glass/polypropylene (E-glass/PP) composite bus seat using extrusion-compression molding. Produced seat from composite presented 43% weight reduction over the steel frame version.

Thattaiparthasarathy et al. (2008) designed and fabricated E-glass/polypropylene (E-glass/PP) composite bus battery box door using the extrusion compression molding process. Produced bus battery box door from composite offered an about weight savings of 60% compared to the steel frame design.

Ning et al. (2007a) designed, manufactured and analyzed a thermoplastic sandwich body panel for a mass transit bus with E-glass fiber/polypropylene (glass/PP) used as the face sheet material and polypropylene (PP) honeycomb used for the core. The authors concluded that the thermoplastic composite body panel weight was 55% lighter than a conventional bus with aluminum skin and supporting steel bars.

Ning et al. (2007b) designed, manufactured and analyzed carbon fiber/Polyphenylene Sulphide thermoplastic (carbon/PPS) composite frame segment (sub-element) of a mass transit bus with three cross-section configurations (rectangular, V-shape and rounded C-shape) and three basic stacking sequences ($[0/90]_6$, $[\pm45/(0/90)_2]s$, and $[\pm45/(0/90)]_3)$[*]. It seemed that the C-shape profile frame

[*] ±45/0/90 refer to the symbolic notation of the sequence of fiber orientation angles. The subscript ‘3’ is the number of plies and the subscript ‘s’ stands for ‘symmetric’.

structure with the stacking sequence of $[0/90]_6^*$ was superior than the others due to pure buckling and torsional buckling analysis.

Ning et al. (2009) designed, manufactured and analyzed an air conditioning cover roof door on a mass transportation bus carried out thermoplastic polyolefin (TPO) as the outer skin and glass mat thermoplastic (GMT) as the inner liner replacement of an existing aluminum mass transportation bus roof door. The authors concluded that the lightweight thermoplastic composite mass transportation bus roof door weight (12.9 kg) was 39% lighter than the baseline aluminum design (21 kg).

Lee et al. (2004) developed one-piece automotive hybrid aluminum/composite drive shaft by considering the optimal stacking sequence of the composite layer due to the thermal stresses between the aluminum tube and the composite layer. The manufactured hybrid aluminum/composite drive shaft ensured only 75% weight reduction in place of the conventional steel drive shaft. The torque capability of the aluminum/composite drive shaft (4320 Nm) was higher than the design value and the fundamental bending natural frequency of the aluminum/composite drive shaft (9390 rpm) was higher than the design specification (9200 rpm).

3. CHASSIS TYPES AND LOADING CONDITIONS

3.1. Chassis Types

Many different vehicle structure types have been used in car chassis over the years. This section presents information on the car chassis types and their characteristics.

3.1.1. The Underfloor Chassis Frame

In the 1920s, when mass production had become well established, the standard car configuration was separate ‘body-on-chassis’ construction. This had certain advantages, including manufacturing flexibility, allowing different body styles to be incorporated easily and providing the ‘chassis’ to be treated as a separate unit incorporating all of the mechanical components. The shape of the chassis frame suited for mounting the semi-elliptic spring on the beam axle suspension system was favored as it divides the body into separate ‘chassis’ and ‘body’ as preferred by manufacturers in the industry at that time. This case also played an additional part in the choice of this construction method.

The underfloor chassis frame regarded as the structure of the car consisted of a roughly flat ‘ladder frame’ as shown in Figure 3.1 (Brown et al., 2002). This chassis incorporated two open section side frames running the full length of vehicle connecting together by open section cross-members running laterally and riveted to the side frames at 90 joints. This frame chassis belongs to a class of structures called ‘grillages’ (Brown et al., 2002).

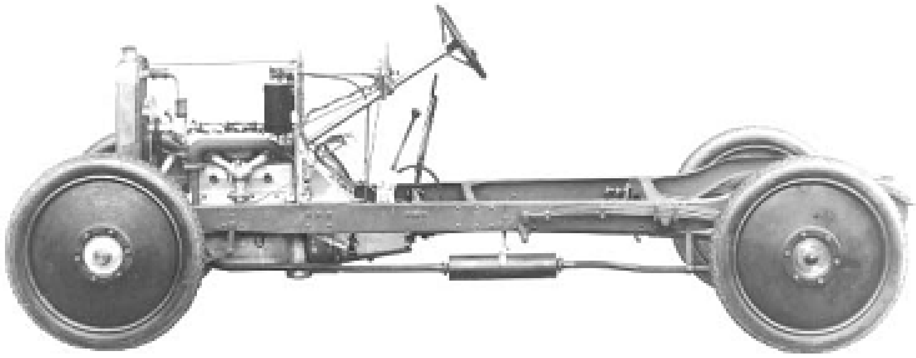

Figure 3.1. Open section ladder frame chassis of the 1920s.

A grillage which is a flat structure subject to the active internal loads.

a) Bending about the in-plane lateral axis of the member.
b) Torsion about the longitudinal axis of the member in the plane of the frame.
c) Shear force in a direction normal to the plane of the frame.

Open section members used for chassis frames in 1920s and 1930s was particularly flexible locally in torsion. Further, the riveted T-joints were poor at transferring bending moments from the ends of members into torsion in the attached members and vice versa. That’s why chassis frames manufactured in that era had very low torsion stiffness. Since, torsion is one of the most important loadings on rough roads, this situation was not very satisfactory. Because of the fact that the depth of the structure was limited to a shallow frame underneath the body, the bending stiffness was not also enough.

A good design carried out by taking into account torsion stiffness is important to ensure road holding of vehicle, to avoid uncalled for vibrations on vehicle and to prevent problems of inconsistency between body and chassis. Torsion stiffness is often used as one of the ‘benchmarks’ of the structural competence of a vehicle structure.

Due to the fact that the majority of car bodies in the 1920s had open bodies which are fundamentally flexible, they had insufficient torsion efficiency of their chassis frame. Car bodies in the 1920s, as shown in Figure 3.2 (Brown et al., 2002), were ‘coach-built’ by carpenters, out of timber, leading to body structures of very low stiffness. At that time, it was commonly assumed that the body experienced none of the road loads (weight of vehicle, passengers and payload etc.). Consequently, it was not designed to be load behavior (particularly for torsion loads) (Brown et al., 2002).

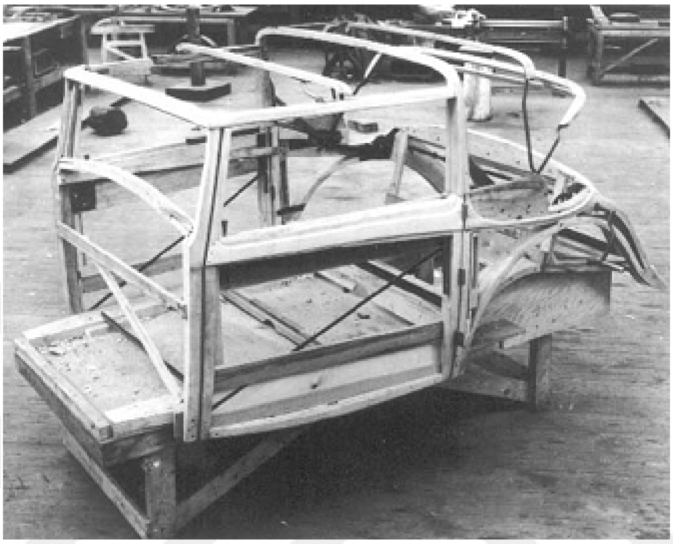

Figure 3.2. Car body manufactured in the 1920s.

Early experience with metal clad bodies led to problems of 'rattling' between the chassis and the body as well as problems of 'squeaking' and 'cracking' at various points within the body which were carrying structural loads. On the basis of these problems lay in the fact that the body and the chassis act like springs in parallel.

For springs in parallel, the load is shared between the springs in proportion to their relative stiffnesses. In the simplified case, the body and the chassis are connected at their ends, as shown in Figure 3.3 (Brown et al., 2002).

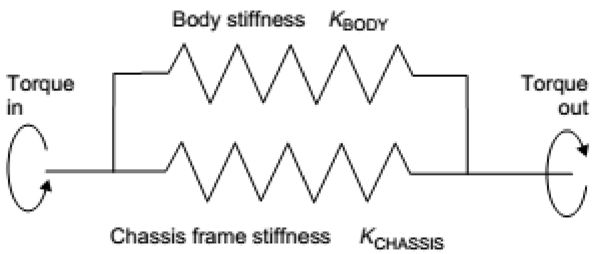

Figure 3.3. Springs in parallel.

$$T_{TOTAL} = T_{BODY} + T_{CHASSIS}$$
$$K_{TOTAL} = K_{BODY} + K_{CHASSIS} \quad (3.1)$$
$$\frac{T_{BODY}}{T_{CHASSIS}} = \frac{K_{BODY}}{K_{CHASSIS}}$$

T = torque, and K = torsional stiffness

According to this, if the body is flexible and the chassis is stiff, then the chassis would carry a larger proportion of the torsion load. Conversely, in the case of a stiff body and a flexible chassis frame, then most of the torsion load would pass through the body.

As the 1920s advanced, this situation was noticed in results of experiences obtained in the construction approach. Bodies were deliberately manufactured to be a flexible structure by the use of flexible metal joints between the resilient timber body members, and by deliberate use of flexible materials for the outer skin of the body, as shown in Figure 3.4 (Brown et al., 2002).

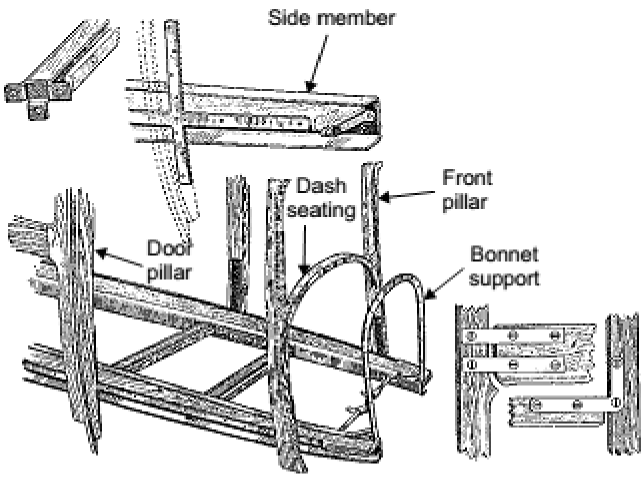

Figure 3.4. Construction details of a timber framed ‘fabric body’.

As the 1920s pass towards the 1930s, the requirements of numerous manufacture gave rise to the commonly utilization of pressed steel car body technology. The bodies were produced by forming out of steel sheets and by welding or riveting together. This entailed much greater stiffness in the body, in particular for torsion, because of the steel panels which were quite effective in shear. The overall configuration still remained as the 'body-on-separate- chassis'.

Although it can be known that a much greater proportion of the load was now taken through the body, due to its greater stiffness, this case gave rise to problems between the body and the chassis frame as rattling or damage to body joints caused by undesirable load transfer between the body and the chassis. To get over these problems, both individually and in combination with each other several approaches were tried. Some of these are presented below:

a) This approach aims at increasing the strength of the chassis. This way, it ensures carrying of more load. Riveted chassis frame technology with open section profile became the standard in the 1930s. However, using open section members was still needed to increase the torsional stiffness. A widespread solution was the use of cruciform bracing. For this, a cross-shaped brace, made usually of open channel section members, was incorporated into the chassis frame as shown in Figure 3.5 (Brown et al., 2002).

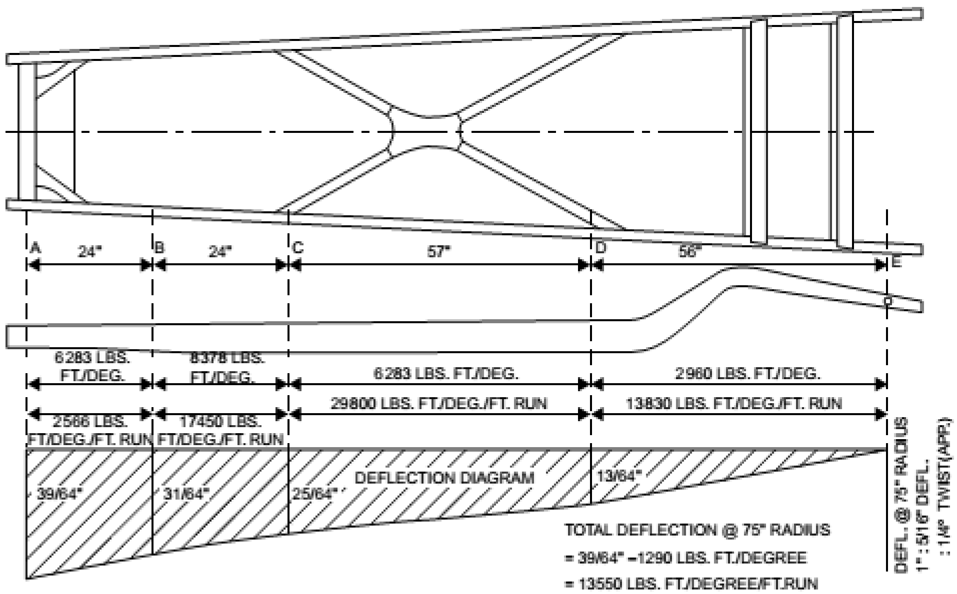

Figure 3.5. Cruciform braced chassis frame.

By the mid-1930s, manufacturing of more durable vehicles against torsion stiffness was began. It was known that gave overall torsion stiffness values between 1000 and 1750 Nm/deg. for various cruciform-braced chassis frames. One of the best of the cruciform braced underfloor open section chassis was that of the Lagonda V12 of the late 1930s, as shown in Figure 3.6 (Anonymous, 2015a).

Figure 3.6. Lagonda V12.

b) Another way of improving chassis frame torsion stiffness was to incorporate closed (i.e. 'box section') cross-members. Closed section members have the more durable torsion stiffness than equivalent open section ones. Car chassis used small closed section cross-members in 1930s gave a considerable increase in torsion compared with previous chassis. However, this chassis was insufficient for torsion stiffness at present time.

c) By the mid-1930s it was realized that the steel body was much stiffer than the chassis in both bending and torsion. Integration of the body with the chassis frame used in some designs was connected by a great number of screws, is shown in Figure 3.7 (Brown et al., 2002). Further, this approach pioneered the modern 'integral body' notion.

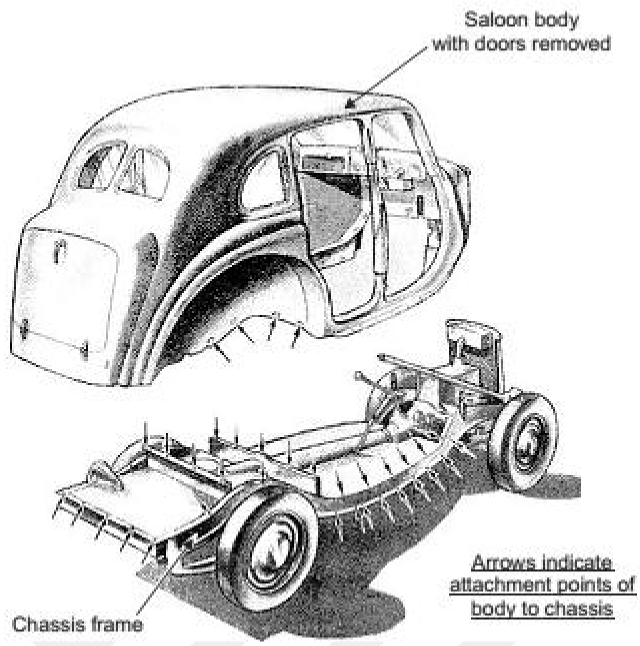

Figure 3.7. Multiple attachments of body to frame

d) The ultimate version of the underfloor chassis frame using small section members is the ‘twin tube’ or ‘multi tube’ frame. This chassis which is a ladder type grillage frame was consisted with side members connected by lateral cross-members. These members were welded together in this construction method. Because of this, the torsion stiffness of the chassis was increased. This type of structure was used in specialist racing vehicles between the late 1930s and the 1950s. For example, the Auto Union racing car (1934–1937), as shown in Figure 3.8 (Brown et al., 2002), used this system, as did many sports racing cars in the 1950s. Moreover, many sports racing cars as Ferrari and Lister Jaguar used this type chassis until 1950s (Brown et al., 2002).

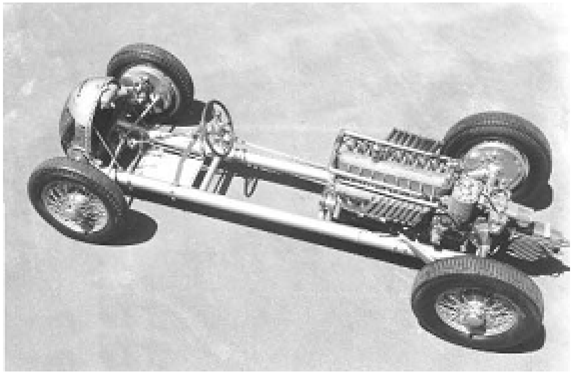

Figure 3.8. Twin tube frame of Auto Union racing car.

3.1.2. Modern Structure Types

In more modern times, the closed tube (or closed box) torsion structure has been used to greater effect by using larger section, but thinner walled members. These structures demonstrated the stiffer against torsion and bending stiffness. It was obtained the development of better road holding, coming from a better understanding of suspension geometry, made greater body stiffness. Welded and pressed sheet steel body technology led to the widespread use of the ‘large section tube’ concept in car structures in the post-World War II era (Brown et al., 2002).

3.1.3. Backbone Structure

This structure is a chassis which has a rectangular section tube like backbone and connects the front and rear axle and provides nearly all the mechanical strength of the chassis. This is used on specialist sports cars like Lotus shown in Figure 3.9 (Anonymous, 2015b).

This chassis frame is separated from the body. The backbone chassis derives its stiffness from the large cross-sectional enclosed area of the ‘backbone’ member which is around 200mm x 150mm size.

Figure 3.9. Sheet steel backbone chassis.

It was seen that the walls of the tube structure subjected to torsion was exposed to shear loads. Although shear panels are not the only way of carrying in-plane shear loads, in the case of the Lotus, the walls of the tube consist of shear panels. A triangulated 'bay' of welded or brazed small tubes had influence in shear loads and this ensured weight saves. This approach is used in some specialist sports cars, such as the TVR shown in Figure 3.10 (Brown et al., 2002).

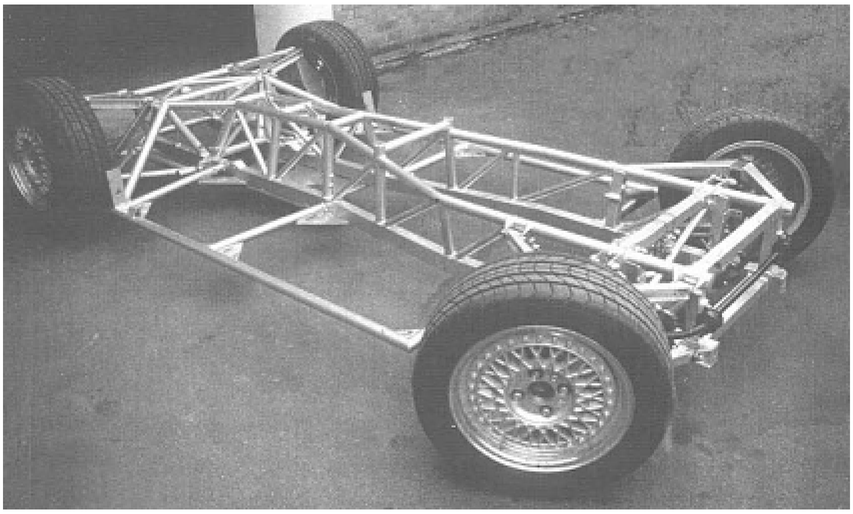

Figure 3.10. Backbone chassis made of triangulated tubes.

Such specialist vehicles often have bodies made of glass reinforced plastic. The body is constructed on the backbone. In most of vehicles of this type, the combined torsion stiffness of the chassis and the attached body together is greater than the sum of the stiffness of the individual items.

Chassis and body connection is not only at the ends, but is made at many points, giving a combined structure. Thus, chassis and body connection behaves as a single piece (Brown et al., 2002).

3.1.4. Triangulated Tube Structure

The triangulated tube structure is not limited to backbone structures. Sports cars with bathtub shaped structure are adapted from this design. Caterham is an example of this structure, as shown in Figure 3.11 (Brown et al., 2002).

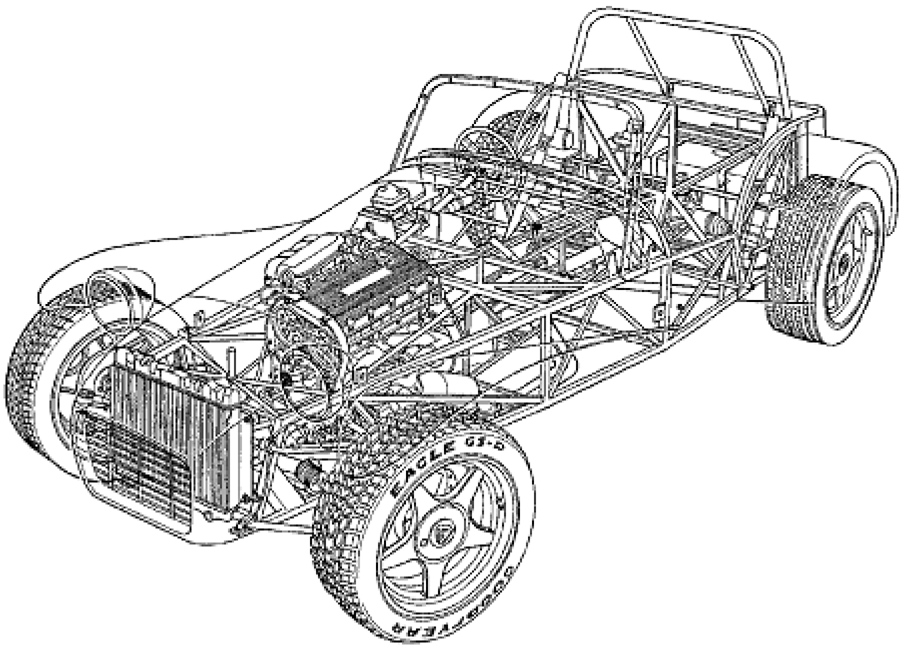

Figure 3.11. Triangulated sports car structure.

This approach has the advantage that the coachwork can consist of thin sheet metal cladding, attached directly to the framework. This method of construction is best suited to low volume production because of low tooling costs. It is not well suited to mass production due to complication and labour intensive manufacture (Brown et al., 2002).

3.1.5. Incorporation of Roll Cage into Structure

Another way of using the tube principle is to implement the tube structure encompassed whole car body. Triangulated sports car structure which is a version of this is shown in Figure 3.12 (Brown et al., 2002).

Figure 3.12. Triangulated sports car structure with integrated roll cage.

The triangulated ‘roll cage’ now extends around the passenger compartment. The larger the enclosed cross sectional area of the body, the larger the torsion constant it can obtain. Since torsion stiffness of this structure is very high, it is used for the more racing vehicles (Brown et al., 2002).

3.1.6. Monocoque

The word monocoque is a French term for "single shell". Monocoque is a structural approach supported through an object’s outer skin, similar to an egg shell (Anonymous, 2015c). Hence the outer skin undertakes the dual role of the body surface and structure. This is the automotive version of aircraft ‘stressed skin’ construction. It is supplied very weight saves.

McLaren was the first company utilizing carbon-fiber-reinforced polymers to construct the monocoque of the McLaren MP4/1, which debuted in 1981. McLaren produced the first F1 car by using a carbon-fiber monocoque in 1992 (Anonymous, 2015c).

The monocoque car structure is relatively rare. Its widespread use is restricted to racing cars as shown in Figure 3.13 (Brown et al., 2002). There are several reasons for this.

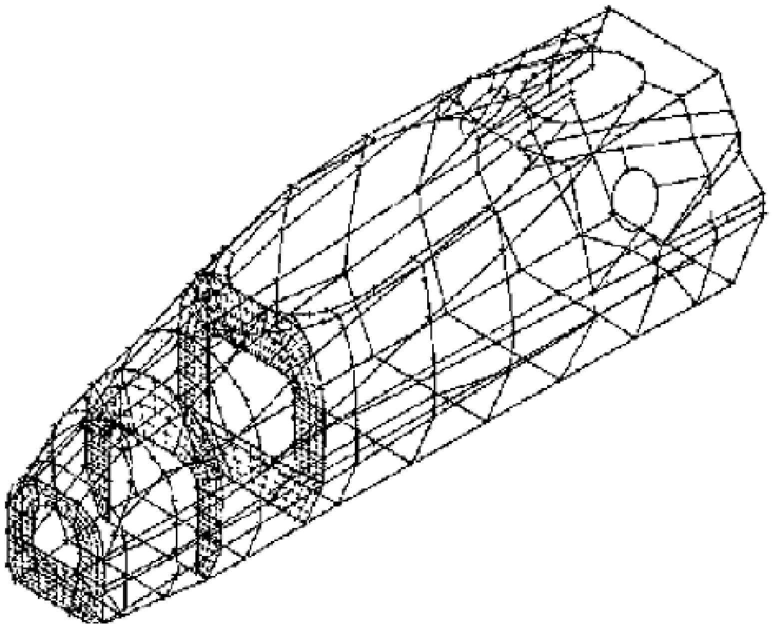

Figure 3.13. Monocoque structure.

First, for the monocoque to run efficiently, it requires its production as a totally closed tube. There are openings for passenger entry, outward visibility, etc. in the practical vehicles. These openings lead to interruptions on the single shell, consequently torsion stiffness of vehicle reduce. Also, the shell requires reinforcement: (a) to prevent buckling and (b) to carry out-of-plane loads.

Typical Formula 1 racing car monocoques is usually made of carbon fibre composite sandwich material and they can reach torsion stiffness greater than 30000 Nm/deg (Brown et al., 2002).

3.1.7. Platform Structure

Other modern car chassis type is the platform structure. This is produced by connecting sheet metal floor members together with large closed section. This structure is a grillage structure with high torsion and bending properties. In many cases, the upper body is handled as structurally insignificant. The platform structure is often used for low production volume vehicles, because of the fact that different body styles, or rapid model changes are required. The Lotus Elise (aluminium, see Figure 3.14 (Anonymous, 2015d)). is an example of a platform structure. This approach is often also used to produce cabriolet or convertible versions of mass produced integral sedan car structures (Brown et al., 2002).

Figure 3.14. Platform Chassis.

3.1.8. Space Frame Structure

Another modern structure is the space frame or 'birdcage' frame. It is a typical example of the Audi A2 aluminum vehicle for this chassis, as seen in Figure 3.15 (Brown et al., 2002).

In this type of structure, small section tubular members are welded in nodes to 'ring-beam' bays. For this, the edges of each ring frame, and especially the corners, must be durable locally in bending.

This choice of production method is usually specified by production needs. After the various beam sections in the production of A2 are produced from extruded or cast aluminum, they must be assembled into this structural design work using welded ‘nodes’ or joints (Brown et al., 2002).

Figure 3.15. Space frame chassis.

3.1.9. Integral or Unitary Body Structure

The ‘integral’ (or ‘unitary’), spot welded, pressed steel sheet metal body is the most widely used modern car structure type suited to mass production methods. The body is self-supporting, so it is not required the separate ‘chassis’ design. Because of this, it is a saving in weight.

The first production in this way was made in the 1930s. A remarkable example was the Citroen 11 CV which was in production from 1934 to 1956 as shown in Figure 3.16 (Anonymous, 2015e).

Figure 3.16. Citroen 11 CV.

The structure was modernized from separate body-on-chassis (1938 model year) to integral construction (1939 model) in a study conducted by Swallow on the Hillman 10 HP vehicle. These structures were compared to the torsional behavior, as shown in Figure 3.17 (Brown et al., 2002). The torsion stiffness increased from 934 Nm/deg. for the chassis and body (together) for the earlier model to 3390 Nm/deg. for the integral body (Brown et al., 2002).

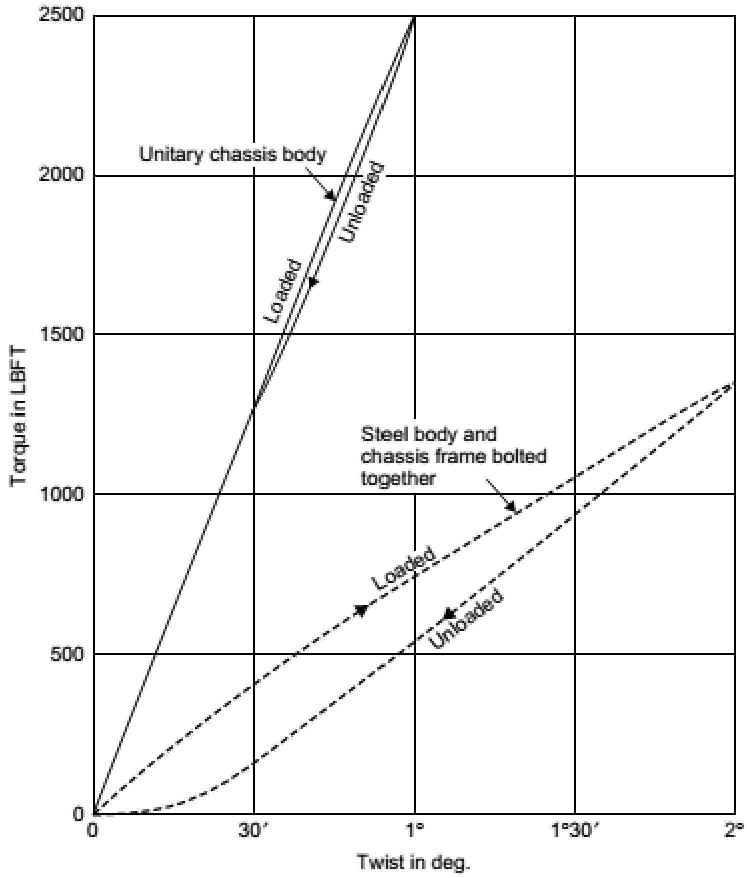

Figure 3.17. Torsion stiffness tests.

Figure 3.18 shows a modern example of an integral 'body-in-white' (Anonymous, 2015f). The integral body is made up of a mixture of the monocoque and the space frame types. The body forms a 'closed box' torsion structure with high stiffness. The walls or surfaces of the box consist of the skin panels (such as the roof, floor, bulkheads, etc.) where possible. Elsewhere open bay ring frames (side frame, windshield frames etc.) form the surface of the box. Beam members in the floor are used to carry out-of-plane loads (Brown et al., 2002).

Figure 3.18. Modern integral body in white.

In the integral structure the panels and body components are fastened from sheet steel and fixed together mostly by spot welding as well as clinching, laser welding or other methods are used for certain locations. The beam members are formed from folded or pressed sheet steel shapes, welded together as shown Figure 3.19 (Brown et al., 2002).

Figure 3.19. Integral body floor assembly.

If properly manufactured, the integral body is well capable of carrying torsion, bending and other loads. Because the structure includes the outer surface of the body, it is much stiffer than most other vehicle structure types, for the reasons given above. Typical values of torsion stiffness for modern integral car bodies are approximately 8000 to 10 000 Nm/deg. for 'everyday' sedans and higher (around 12 000 to 15 000 Nm/deg. or more) for luxury vehicles (Brown et al., 2002).

3.2. Chassis Loading Types

A chassis is subjected to various loads due to uneven road surfaces and a plain road. These loads are transmitted from the reaction forces of the wheels due to road undulations to the chassis. These loads applied by aid of finite element analysis in the simulation program are roughly simplifications of actual complex road loading situations. The simplified loads are applied on the chassis in the preliminary design stage. This process involves to measurement of the chassis usage on applicable geographic regions and provides convenience to the designer. Obtained data help to create, modify or update designer providing road cases to better use of the chassis of the customer (Brown et al., 2002b). So the chassis should be designed and construct to maximize payload capability and to provide sophistication, durability as well as sufficient performance (Bhaskar et al., 2014). It is important to understand the different loads acting on the structure in designing the chassis. The some deformation modes for an automotive chassis are given below (Riley and George, 2002).

1. Vertical symmetrical (Bending Case)
2. Vertical asymmetric (Torsion Case)
3. Lateral bending (Cornering)

3.2.1. Vertical Symmetric Load Case

This load case consists of when both wheels on one axle of the vehicle encounter a symmetrical bump simultaneously as shown in Figure 3.20 (Brown et al., 2002b). This leads to a bending moment effect on the chassis about a lateral axis (Brown et al., 2002b).

Figure 3.20. Vertical Symmetric Load Case.

The weight of driver, passenger, engine, battery etc. under an impact of gravity occur collapse in the chassis as shown in Figure 3.21 (Singh, 2010). Chassis is assumed to act as simply supported beam and four wheels as supports tend to occur reactions vertically upward at the axles (Singh, 2010).

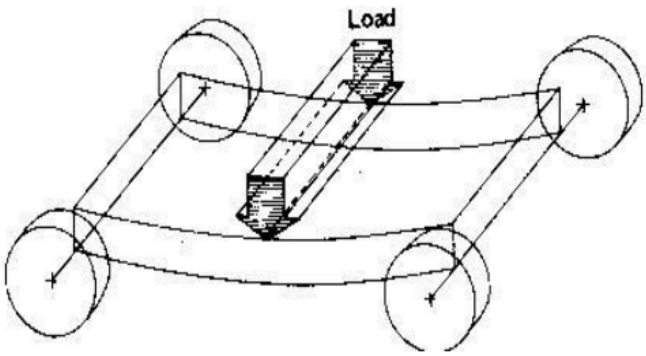

Figure 3.21. Vertical Bending Case.

3.2.2. Vertical Asymmetric Load Case

Vertical asymmetric loading occurs when only one wheel on an axle passes over a bump as shown in Figure 3.22 (Brown et al., 2002b). This load case applies torsion as well as bending on the vehicle chassis.

Figure 3.22. Vertical Asymmetric Load Case.

Torsional loads came from an undulating road surface are one of the most important and highest magnitude loads transmitted through the chassis (Riley and George, 2002). Further, torsion stiffness is an important characteristic in the chassis design with an influence on the handling and the performance of the vehicle. It is important for the chassis design to increase the torsion stiffness without greatly increasing the weight of the chassis (Tebby et al., 2011). To analyze the torsional ridity of a chassis, the rear end of the chassis is fixed and equal and opposite loads are applied at the front end of the chassis. When this concept applied to the real chassis would look like Figure 3.23 (Riley and George, 2002).

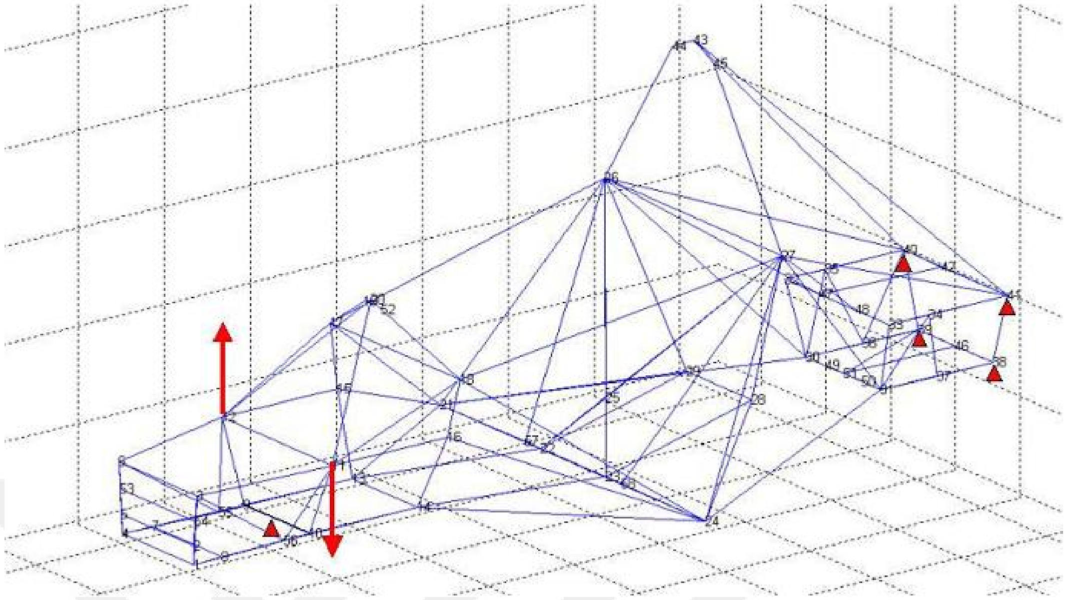

Figure 3.23. Chassis Finite Element Model Loading Case.

The resistance to torsional deformation is named as stiffness and it is expressed in Nm/degree in SI units. The torsional ridity can be calculated by finding the torque applied to the chassis and dividing by the angular deflection, as shown in Figure 3.24 (Riley and George, 2002).

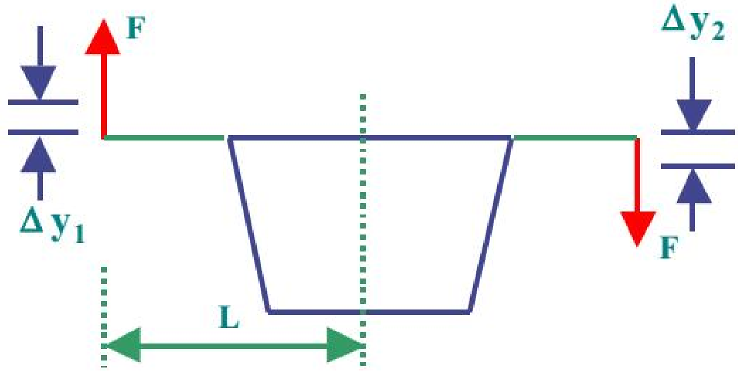

Figure 3.24. Front Suspension Bay Testing Loads.

The torsional stiffness is calculated as;

$$K = \frac{T}{q} \tag{3.2}$$

$$K = \frac{FL}{\tan^{-1}\left[(\Delta y_1 + \Delta y_2) / 2L \right]} \tag{3.3}$$

In the above equations;

K: Torsional Stiffness [Nm/degree]

T: Torsion Moment (Torque) [Nm]

ϴ: Torsion Angle (The Angular Deflection) [˚]

F: Vertical Force [N]

L: Width of The Vehicle [mm]

Δy_1: Displacement at Left Side

Δy_2: Displacement at Right Side

3.2.3. Lateral Load Case

Lateral load case occurs mainly due to the centrifugal forces caused by cornering, road camber and side wind forces on the chassis. These loads act along the length of chassis and is resisted by axles, tires and side impact members etc. as shown in Figure 3.25 (Singh, 2010).

The chassis is fixed to the parts that are connected to the chassis of the wheel and acceleration in the direction of the bend has been occurred on the car.

The centripetal acceleration is calculated as;

$$a_C = \frac{V^2}{r} \tag{3.4}$$

where a_C is the centripetal acceleration

r: horizontal bend radius

V: vehicle’s speed

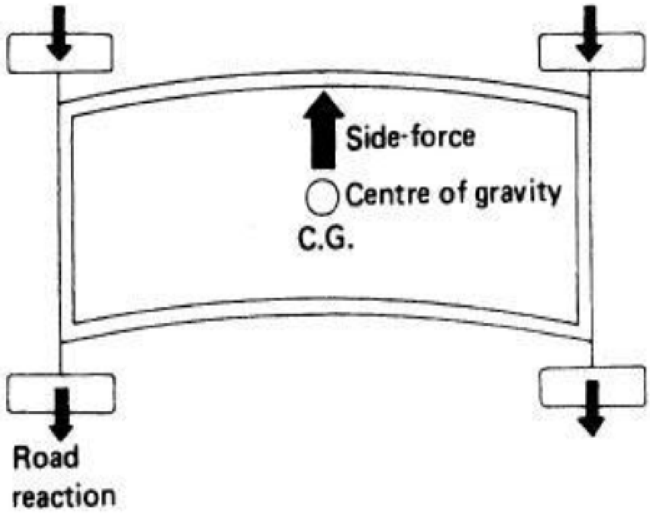

Figure 3.25. Lateral Bending Case.

4. MATERIAL AND METHOD

4.1. Materials

4.1.1. Composite Materials

In this study, unidirectional-300g/m^2 carbon fiber fabrics and laminating resin MGS L160 epoxy are used to manufacture polymer matrix composite material. The epoxy and the carbon fiber materials are used as a matrix and reinforcement constituent, respectively. These materials were supplied by Dost-kimya-company. The mechanical and physical properties of these materials are listed in Table 4.1.

Table 4.1. Mechanical and physical properties of materials

Materials	Tensile strength (MPa)	Young's modulus (GPa)	Density (g/cm^3)	Diameter (µm)
Carbon Fiber	4900	240	1,79	7
Epoxy	70-80	3,2-3,5	1,13-1,17	-

4.1.2. Production of Laminated Composite Materials

All the laminated composite materials used in the experimental work are prepared with the aid of a vacuum infusion technique at the Laboratory of Mechanical Engineering in Adana Science and Technology University Laminating resin MGS L160 epoxy and laminating hardener H160 were mixed with the volume fraction of 100:30 for matrix material. For optimum properties, laminated composite material samples are produced with the help of vacuum infusion technique kept in room temperature for 24h under 1 atm pressure, then post-cured at 50˚C for 12h in the electric furnace, as seen in Figure 4.1.

Figure 4.1. Preparation laminated composite material samples with the aid of a vacuum infusion techniques.

Following the cure process, laminated composite materials are cut with the help of CNC water jet cutting machine in dimensions required according to ASTM standard test methods, as shown in Figure 4.2.

Figure 4.2. Cutting the specimens with the help of CNC water jet cutting machine as required by the ASTM standard test methods.

4.2. Experimental Method

The purpose of this chapter is to briefly review the most commonly used methods for mechanical testing of composite materials and their constituents. Much of our knowledge about the special nature of composite behavior has been derived from experimental observations. The measurement of mechanical properties is also an important element of the quality control and quality assurance processes associated with the manufacture of composite materials and structures. Due to the special characteristics of composites, such as anisotropy, coupling effects and the variety of possible failure modes, it has been found that the mechanical test methods that are used for conventional metallic materials are usually not applicable to composites. Thus, the development and evaluation of new test methods for composites has been, and continues to be, a major challenge for the experimental mechanics community. The technology associated with composite test methods and test equipment has become just as sophisticated as that associated with the corresponding analytical methods. Many of these test methods have evolved into standards which have been adopted by the American Society for Testing and Materials (ASTM) (Gibson, 1994).

Nine independent elastic constants are required to define the mechanical response of an orthotropic lamina (Staab, 1999). The determination of basic material properties of unidirectional laminated composite plate under static loading conditions using experimental method has always been a key issue in the research on composite materials. With the rise of huge variety of composites, the need for an efficient and reliable way of measuring these properties has become more important. The experiments, if conducted properly, generally reveal both strengths and stiffness characteristics of the material (Jones,1998).

The strengths characteristics are,

X : Axial or longitudinal strength (1 direction)

Y : Transverse strength (2 direction)

S : Shear strength (1-2 plane)

The stiffness characteristics are,

E_1 : Young’s modulus in the 1-direction(Longitudinal)

E_2 : Young’s modulus in the 2-direction (Transverse)

ν_{12} : Poisson’s ratio

G_{12} : Shear modulus in 1-2 coordinates

The directions of these strengths are shown in Figure 4.3.

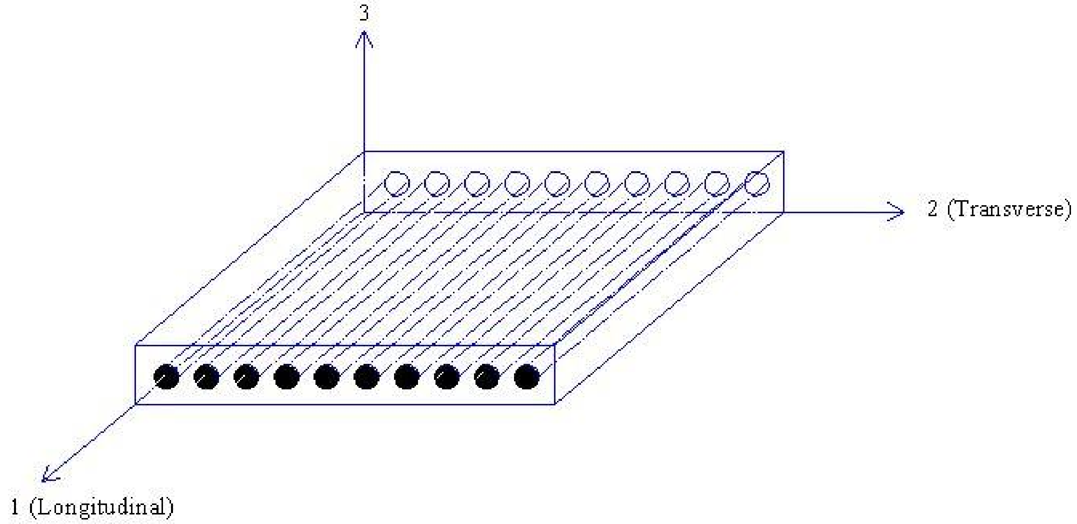

Figure 4.3. The directions of fundamental strengths for a unidirectional reinforced lamina.

4.2.1. Experimental Process

All the experiments are carried out using Shimadzu AGS-X WITH CLASS 0.5 100kNloadcell Test Machine in Mechanic Laboratory at Adana Science and Technology University. The required basic material properties are estimated under five primary loading modes that are tension, compression, notched compression, bending and in-plane shear. The geometries and standards of the test specimen are illustrated in Table 4.2 (Gibson, 1994; Jones, 1998; Okutan, 2001).

Table 4.2. Geometries of the experiment specimens

Determinable properties	**Symbol and Unit**	**ASTM test method**	**Specimen geometry**
Axial or longitudinal modulus Axial Poisson's ratio Longitudinal tensile strength	$E_1\ (MPa)$ n_{12} (-) $X_t\ (MPa)$	ASTM D3039M-00	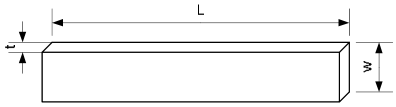
Transverse modulus Transverse Poisson's ratio Transverse tensile strength	$E_2\ (MPa)$ n_{21} (-) $Y_t\ (MPa)$		
Longitudinal Flexural Strength Longitudinal Flexural Modulus	$s_f^L\ (MPa)$ $E_B^L\ (MPa)$	ASTM D790-02	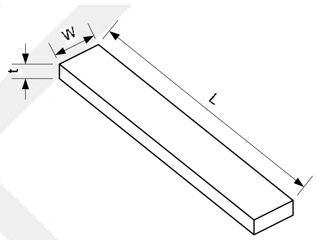
Transverse Flexural Strength Transverse Flexural Modulus	$s_f^T\ (MPa)$ $E_B^T\ (MPa)$		
Longitudinal Compressive Strength Longitudinal Compressive Modulus	$X_C\ (MPa)$ $E_{11}^C\ (MPa)$	ASTM D3410M-03	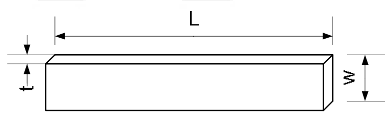
Transverse Compressive Strength Transverse Compressive Modulus	$Y_C\ (MPa)$ $E_{22}^C\ (MPa)$		
Shear modulus Shear strength	$G_{12}\ (MPa)$ $S_{12}\ (MPa)$	ASTM D5379M-98	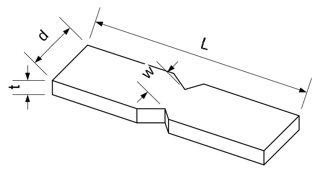
Open Hole Compressive Strength	$F^{ohcu}\ (MPa)$	ASTM D6484M-04	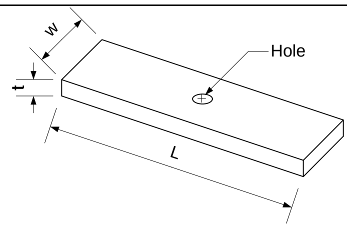

4.2.2. Density Specification Test

The density of each specimen is measured in accordance with the ASTM D792-00 Standard Test Methods for density and specific gravity (Relative Density) of plastics by displacement. Figure 4.4.shows weighing by means of a pair of scales of the specimen.

Calculate the density of a composite material as follows:

$$\rho_c = \frac{W_a}{W_a + W_w - W_b} \times \rho_{water} \qquad (4.1.)$$

where:

ρ_c = the density of the composite material, in g/cm^3

W_a = apparent mass of specimen in air.

W_w = apparent mass of totally immersed sinker and of partially immersed wire.

W_b = apparent mass of specimen completely immersed and of the wire partially immersed in liquid.

ρ_{water} = the density in g/cm^3 of water at testing temperature (0,9975 g/cm^3 at 23˚C)

To obtain the mean value of density of five specimens, each specimen is tested.

Figure 4.4. Weighing by means of a pair of scales of the specimen

4.2.3. Fiber Volume Fraction Measurement

The fiber volume fraction is one of the main parameters in the determination of the composite's mechanical properties. The fiber volume fraction can be experimentally determined by the ignition loss method or the matrix burn-off test (ASTM D2584).

The matrix burn-off tests are performed according to the ASTM D2584-02 Standard Test Method for Ignition Loss of Cured Reinforced Resins to measure the carbon fiber volume fraction (V_f). In this method, a small sample of composite is heated in a porcelain crucible until the epoxy matrix ignites in an electric muffle furnace reaching up to 450˚C(Figure 4.5.). This furnace temperature is sufficient to remove the carbon fiber, although the ASTM D2584 standard recommends a furnace temperature of 565˚C. This composite specimen is separated from the resin portion of a weighed composite specimen in a hot furnace medium. The residue is filtered and weighed. The weight percent of fiber could be converted to a volume percent of by using the fiber and resin densities. The fiber volume fraction of specimens is estimated with at least five samples. Figure 4.6.shows unidirectional carbon fiber fabric in a porcelain crucible after burning off in electric muffle furnace.

Figure 4.5. An electric muffle furnace.

Figure 4.6. Unidirectional carbon fiber fabric in a porcelain crucible after burning off.

The fiber volume fraction is calculated according to the ASTM D2584 standard as follows:

$$V_f = \left[\frac{\rho_m \times W_f}{(\rho_m \times W_f) + (\rho_f \times W_m)} \right] \quad (4.2.)$$

where V_f was the fiber volume fraction, W_f was the weight of fiber, W_m was the weight of matrix, ρ_f was the density of fiber and ρ_m was the density of matrix.

4.2.4. Tensile Test

The tensile properties of carbon fiber-epoxy laminated composite specimens, such as longitudinal tensile strength (X_t), transverse tensile strength (Y_t), longitudinal tensile modulus (E_{11}), transverse modulus (E_{22}) and Poisson's ratio (ν_{12},ν_{21}) are determined by practicing static tension testing in longitudinal $[0^0]_4$ and transverse $[90^0]_7$ unidirectional specimens in accordance with ASTM D3039M-00 Standard Test Method for Tensile Properties of Polymer Matrix Composite Plates. The tensile specimen is straight-sided and has a constant cross section. As shown in Figure 4.7., the nominal dimensions of all the specimens to find the longitudinal tensile properties consist of four plies in 0˚ direction where are 250 mm in length,15 mm in width. The nominal dimensions of all the specimens to find the transverse tensile properties consist of seven plies in 90˚ direction where are 175 mm in length,25 mm in width. At least 5 samples were tested for the longitudinal and transverse tensile properties.

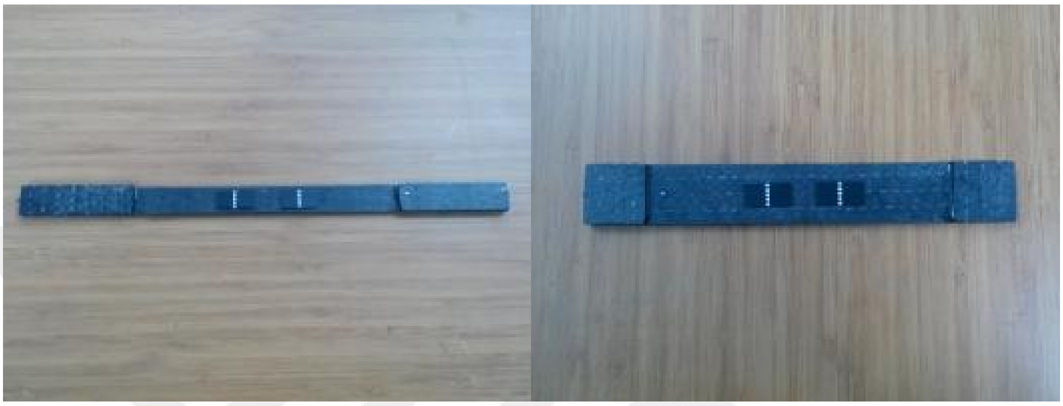

(a) (b)

Figure 4.7. Tensile test specimens (a)the specimen in 0˚ direction,(b)the specimen in 90˚ direction.

The specimens were tested at room temperature using mechanical test machine (Shimadzu AGS-X with class 0.5 100kN loadcell) at a cross head speed of 2 mm/min (Figure 4.8.a-b).

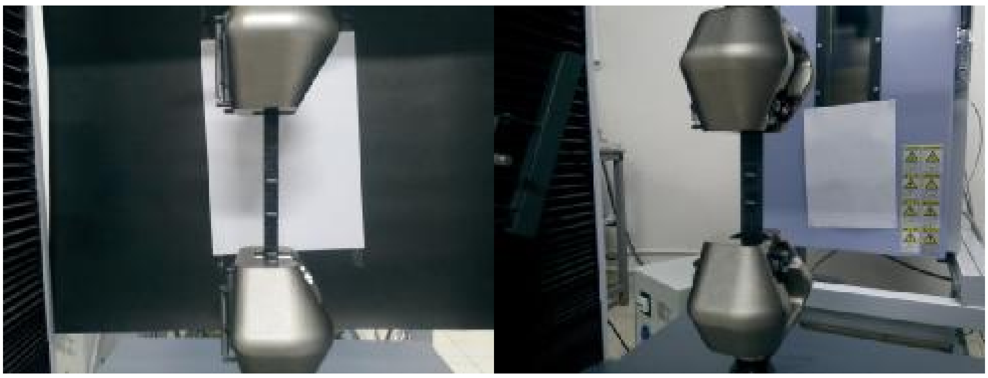

(a) (b)

Figure 4.8. (a)and(b) are shown tensile test specimens during test in 0˚ and 90˚ directions, respectively.

The magnitudes of E_{11},E_{22}, ν_{12} ,ν_{21} and X_t, Y_t are calculated using the tension test data and equations in Table4.3.

Table 4.3. Calculations in tensile test

Mechanical properties	**Symbol and Unit**	**Calculation**	**ASTM test method**
Axial or longitudinal modulus	E_{11} (MPa)	$\sigma_1 = \frac{P}{A}$ $E_{11} = \frac{\sigma_1}{\varepsilon_1}$	ASTM D3039M-00
Axial Poisson's ratio	v_{12} (-)	$\nu_{12} = -\frac{\varepsilon_2}{\varepsilon_1}$	
Longitudinal tensile strength	X_t (MPa)	$X_t = \frac{P_{ult}}{A}$	
Transverse modulus	E_{22} (MPa)	$E_{22} = \frac{\sigma_2}{\varepsilon_2}$	
Transverse Poisson's ratio	v_{21} (-)	$\nu_{21} = \nu_{12}\left(\frac{E_{22}}{E_{11}}\right)$	
Transverse tensile strength	Y_t MPa)	$Y_t = \frac{P_{ult}}{A}$	

In Table 4.3, A is the cross-sectional area of the specimen and perpendicular to the applied load.

Typical load-elongation curves for these tested specimens under static tensile loading are shown in Figure 4.9 and Figure 4.10.

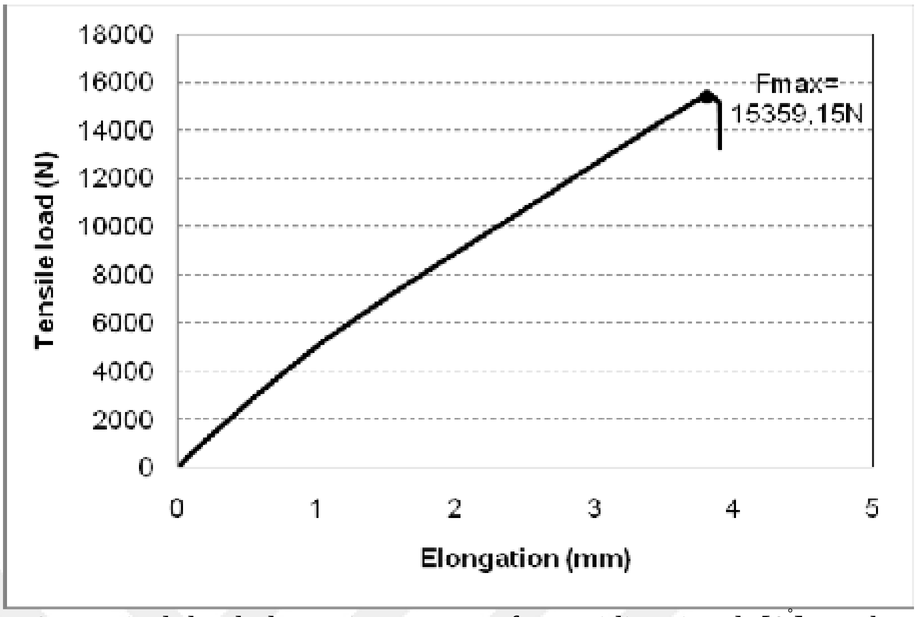

Figure 4.9. Typical load-elongation curve of a unidirectional $[0^{\circ}]_4$ carbon/epoxy specimen under static tensile loading.

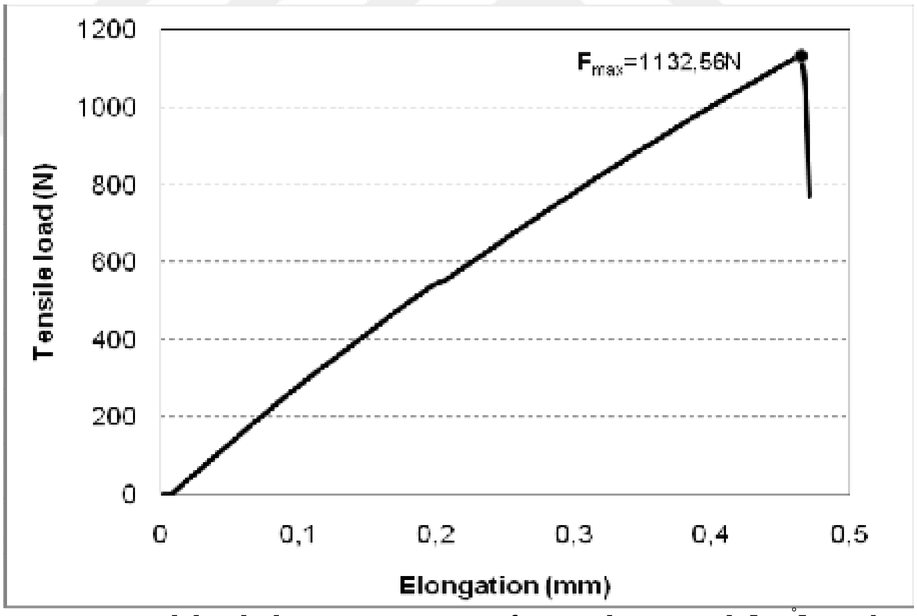

Figure 4.10. Typical load-elongation curve of a unidirectional $[90^{\circ}]_7$ carbon/epoxy specimen under static tensile loading.

4.2.5. Flexural Test

The flexural test method was used to measure the flexural strength and modulus of the composite in accordance with ASTM D790-02 Standard Test Methods for Flexural Properties of Unreinforced and Reinforced Plastics and Electrical Insulating Materials.

In this test method, test specimen is unidirectional as tensile tests and it has a constant cross section. As shown in Figure 4.11., the nominal dimensions of all the specimens to find the flexural properties consist of sixteen plies in 0˚ and 90˚ directions, 100 mm in length and 15 mm in width. At least 5 samples are tested for the flexural properties.

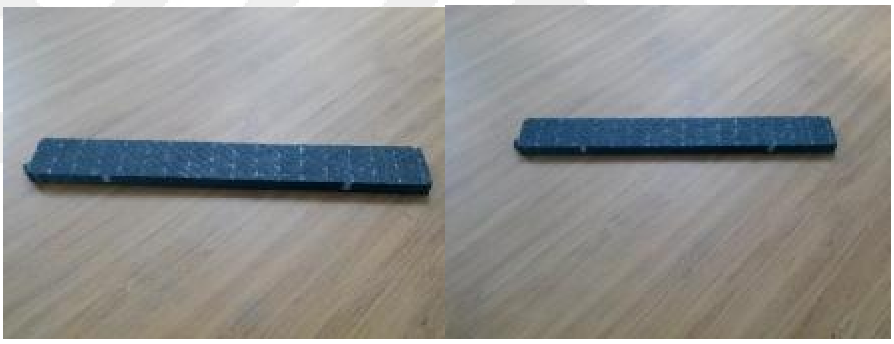

(a) (b)

Figure 4.11. Flexural test specimens (a)the specimen in 0˚ direction,(b)the specimen in 90 direction.

The specimens were tested at room temperature using mechanical test machine (Shimadzu AGS-X with class 0.5 100kN loadcell) at a cross head speed of 1,856 mm/min. In this test, a composite beam specimen of rectangular cross section is loaded in a three-point bending mode (Figure 4.12.).

Figure 4.12. Flexural test specimen during test

It is calculated the rate of crosshead motion by the following formula and set the machine for the rate of crosshead motion, as calculated by Equation4.3.

$$R = \frac{ZL^2}{6d} \qquad (4.3.)$$

where:

R= rate of crosshead motion, mm/min

L= support span, mm

d= depth of beam, mm

Z = rate of straining of the outer fiber, mm/min

The flexural strength (σ_f) in the units of MPa is calculated using the following Equation4.4;

$$\sigma_f = \frac{3PL}{2bd^2} \qquad (4.4.)$$

where:
P = load at a given point on the load-deflection cure, N
L = support span, mm
b = width of the specimen tested, mm
d = thickness of the specimen tested, mm

The flexural modulus of elasticity values $\left(E_B\right)$ are calculated using the following equation 4.5;

$$E_B = \frac{L^3 m}{4bd^3} \tag{4.5.}$$

where:
E_B = modulus of elasticity in bending, MPa
L = support span, mm
b = width of the specimen tested, mm
d = thickness of the specimen tested, mm
m = slope of the tangent to the initial straight-line portion of the load-deflection curve, N/mm

Typical load-deflection curves for these tested specimens under static loading are shown in Figure 4.13 and Figure 4.14.

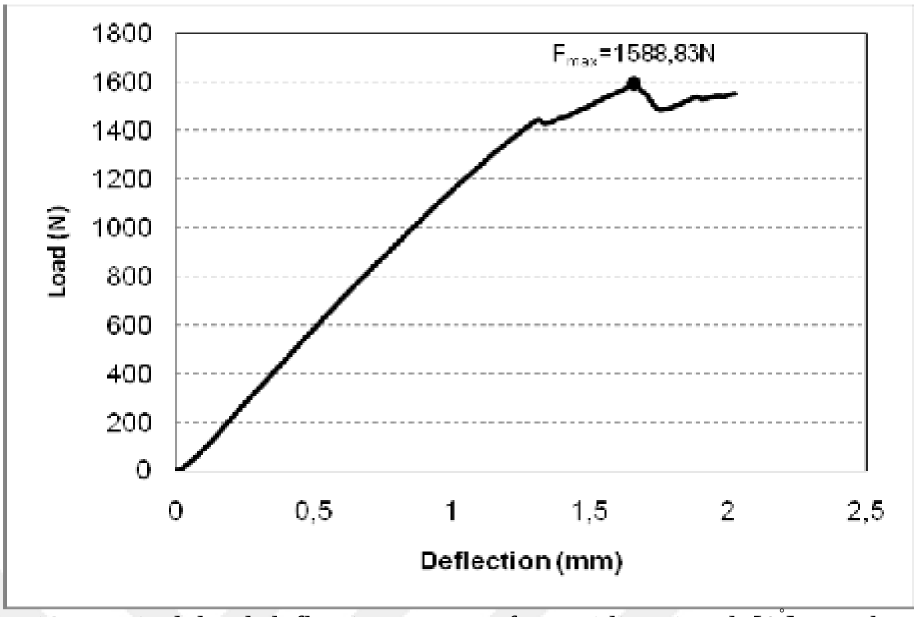

Figure 4.13. Typical load-deflection curve of a unidirectional $[0^{\circ}]_{16}$ carbon/epoxy specimen under static loading.

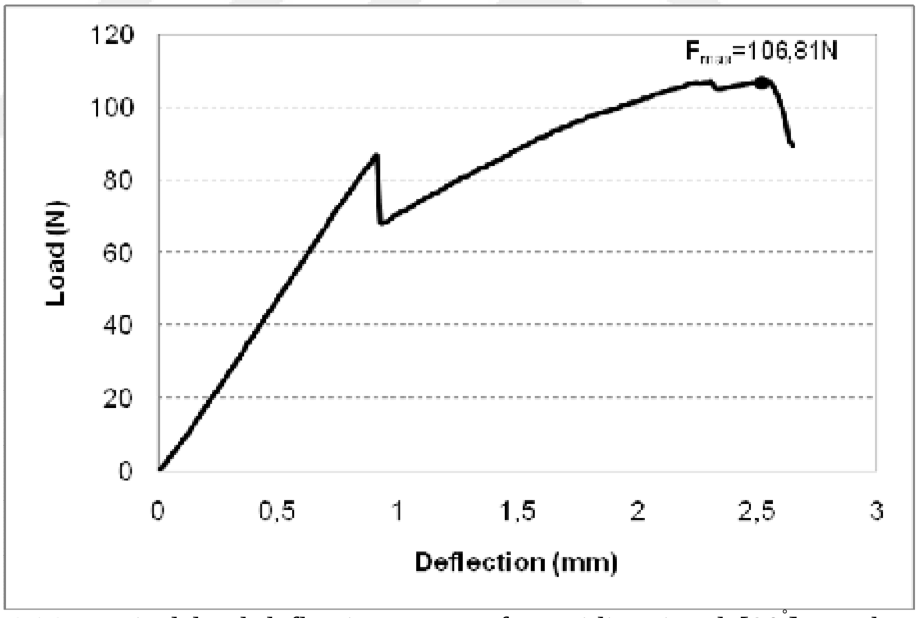

Figure 4.14. Typical load-deflection curve of a unidirectional $[90^{\circ}]_{16}$ carbon/epoxy specimen under static loading.

4.2.6. Compression Test

Compression test method according to ASTM D3410M-03 Standard Test Method for Compressive Properties of Polymer Matrix Composite Materials with

Unsupported Gage Section by Shear Loading is designed to produce compressive property data for material specifications, research, development, quality assurance, structural design and analysis.

This test method is used to measure compressive modulus of elasticity, longitudinal compressive strength (X_C), transverse compressive strength (Y_C) values of the composite plate fabricated from carbon fiber/epoxy unidirectional fabrics. In this test method, test specimen is unidirectional as tensile tests and it has a constant cross section. As shown in Figure 4.15., the nominal dimensions of all the specimens to find the longitudinal compressive properties consist of six plies in 0˚ direction where are 150 mm in length, 10 mm in width. The nominal dimensions of all the specimens to find the transverse compressive properties consist of six plies in 90˚ direction, 150 mm in length and 25 mm in width. At least 5 samples were tested for the longitudinal and transverse compressive properties.

Figure 4.15. Compression test specimen

The specimens are tested at room temperature using mechanical test machine (Shimadzu AGS-X with class 0.5 100kN load cell) at a cross head speed of 1,5 mm/min(Figure 4.16).

Figure 4.16. Compressive test specimen under compression load.

The magnitudes of E_{11}^{C} , E_{22}^{C} and X_C , Y_C are calculated using the tension test data and equations in Table4.4.

Table 4.4. Calculations in compression test

Mechanical properties	**Symbol and Unit**	**Calculation**	**ASTM test method**
Longitudinal compressive modulus	E_{11}^{C} (MPa)	$E_{11}^{C}=\frac{\sigma_1}{\varepsilon_1}$	ASTM D3410M-03
Transverse compressive modulus	E_{22}^{C} (MPa)	$E_{22}^{C}=\frac{\sigma_2}{\varepsilon_2}$	
Longitudinal compressive strength	X_C (MPa)	$X_C=\frac{P_{ult}}{A}$	
Transverse compressive strength	Y_C (MPa)	$Y_C=\frac{P_{ult}}{A}$	

Typical load-deflection curves for these tested specimens under static loading are shown in Figure 4.17 and Figure 4.18.

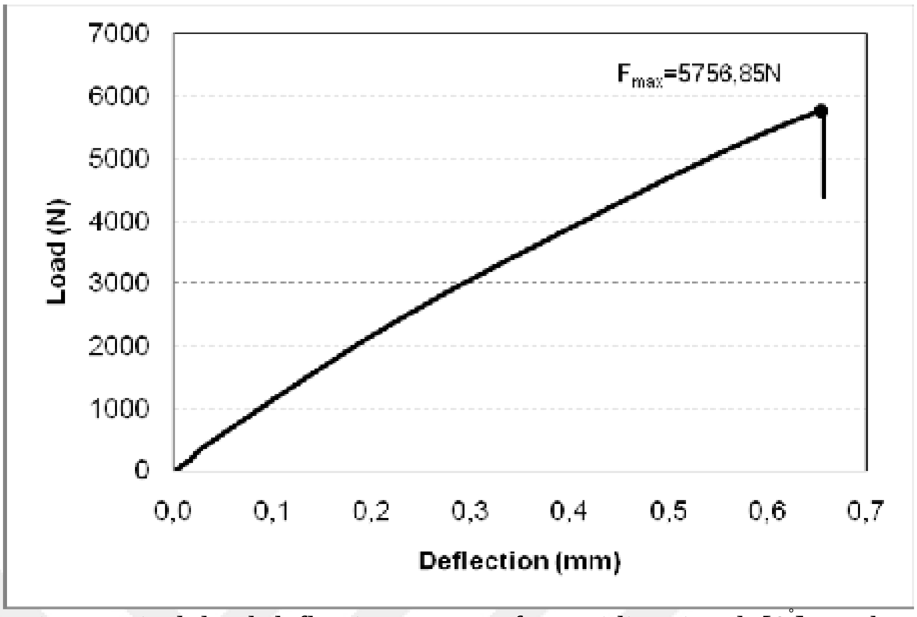

Figure 4.17. Typical load-deflection curve of a unidirectional $[0^{\circ}]_6$ carbon/epoxy specimen under static loading.

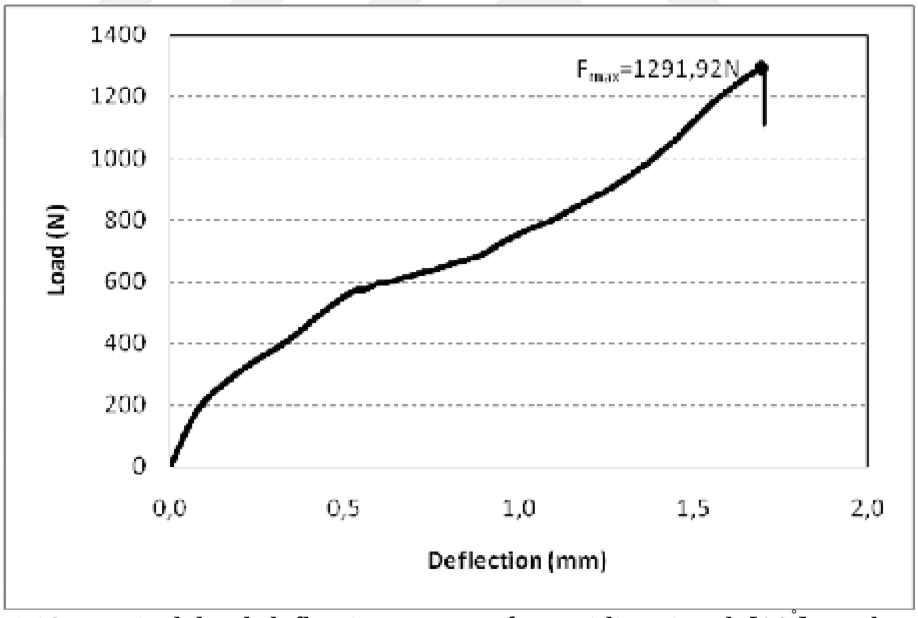

Figure 4.18. Typical load-deflection curve of a unidirectional $[90^{\circ}]_6$ carbon/epoxy specimen under static loading.

4.2.7. The Iosipescu Shear Test

The Iosipescu shear test was originally developed by Nicolai Iosipescu for shear testing of isotropic materials and was later adopted by Walrath and Adams

(1983) for determining the shear strength and modulus of fiber-reinforced composites (Mallick, 1993). This test method is used to measure the shear strength and modulus of the composite in accordance with ASTM D5379M-98 Standard Test Method for Shear Properties of Composite Materials by the V-Notched Beam Method.

In this test method, test specimen is unidirectional as tensile tests and it has a constant cross section. As shown in Figure 4.19, the nominal dimensions of all the specimens to find the shear properties consist of twelve plies in 0˚ and 90˚ directions, 76 mm in length and 20 mm in width. At least 5 samples are tested for the shear properties in 0˚ and 90˚ directions. The specimens were tested at room temperature using mechanical test machine (Shimadzu AGS-X with class 0.5 100kN loadcell) at a cross head speed of 2 mm/min (Figure 4.20).

Figure 4.19. The Iosipescu shear test specimen

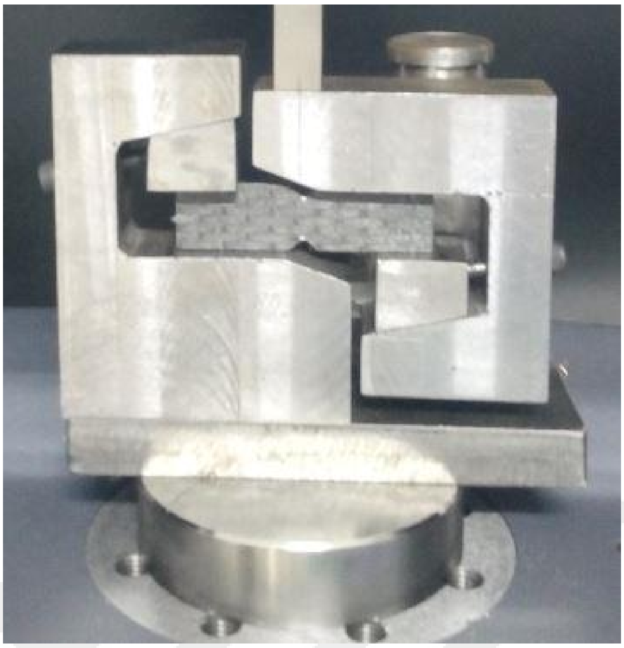

Figure 4.20. A standard V-notched beam test specimen under shear load applied till fracture of the test specimen occurs.

The shear strength (τ_{12}) in the units of MPa is calculated using the following equation;

$$\tau_{12} = \frac{P}{w \times h} \tag{4.6.}$$

where:

P = applied load

w = distance between the notches

h = specimen thickness

The shear modulus of elasticity value (G_{12})in the units of GPa is calculated using the following equation;

$$G_{12} = \frac{\Delta\tau}{\Delta\gamma} \tag{4.7.}$$

where:

$\Delta\tau$ = difference in applied shear stress between the two strain points

$\Delta\gamma$ = difference between the two strain points

Typical load-displacement curves for these tested specimens during the shear test are shown in Figure 4.21 and Figure 4.22.

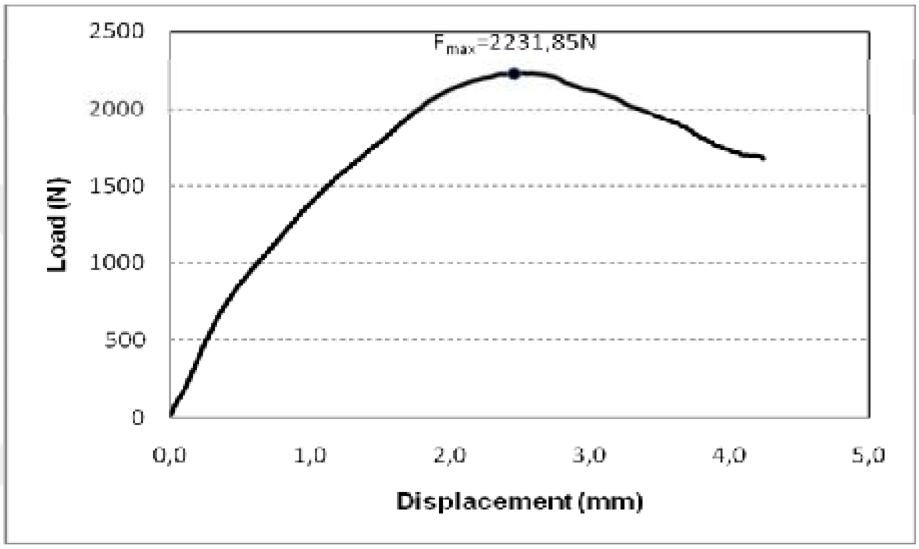

Figure 4.21. Typical load-displacement curve of a unidirectional $[0^{\circ}]_{12}$carbon/epoxy specimen for Iosipescu test specimens.

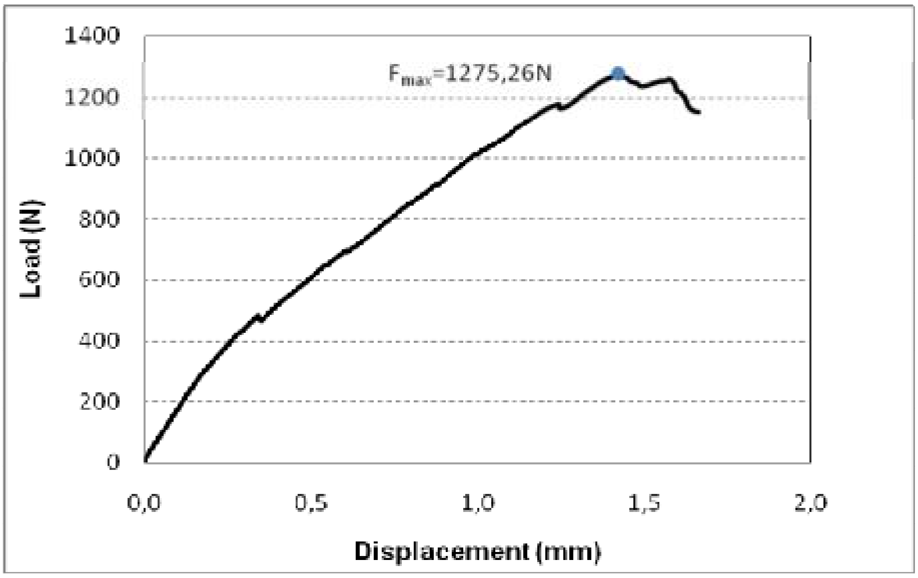

Figure 4.22. Typical load-displacement curve of a unidirectional $[90^{\circ}]_{12}$carbon/epoxy specimen for Iosipescu test specimens.

4.2.8. Open-Hole Compression Test

This test method is used to measure the ultimate open-hole compressive strength of the composite in accordance with ASTM D6484M-04 Standard Test Method for Open-Hole Compressive Strength of Polymer Matrix Composite Laminates.

The open-hole compressive (OHC) specimens in this test method are fabricated using carbon fiber/epoxy in UD carbon fiber fabric form and the specimen geometry in ASTM D6484. For each specimen fabricated, sixteen UD carbon fiber fabric plies are tailored and stacked in multidirectional fiber orientations. The multidirectional plies had the stacking sequence of $\left[45^{0}_{2}/\text{-}45^{0}_{2}/0^{0}_{2}/90^{0}_{2}\right]_{s}$. At least 5 samples are tested for the open-hole compressive properties. As shown in Figure 4.23, the specimens with a thickness of 4.52 mm are used for OHC testing with the dimensions of 300 mm in length and 36 mm width with 6 mm hole (drilled in the center). The specimens are tested at room temperature using mechanical test machine (Shimadzu AGS-X with class 0.5 100kN loadcell) at a cross head speed of 2 mm/min (Figure 4.24).

Figure 4.23. Open hole test specimen

Figure 4.24. A standard open-hole compressive test specimen under compression load.

The open-hole compressive strength (F^{ohcu}) in the units of MPa is calculated using the following equation;

$$F^{ohcu} = P_{\max} / (h \times w) \tag{4.8.}$$

where:

F^{ohcu}= ultimate open-hole compressive strength, MPa

P_{max} = maximum force prior to failure, N

A = the cross-sectional area (disregarding hole) = h x w, mm^2

Figure 4.25 shows typical load-displacement curve of a multidirectional $\left[45^0_2/\text{-}45^0_2/0^0_2/90^0_2\right]_s$ carbon/epoxy specimen during OHC test.

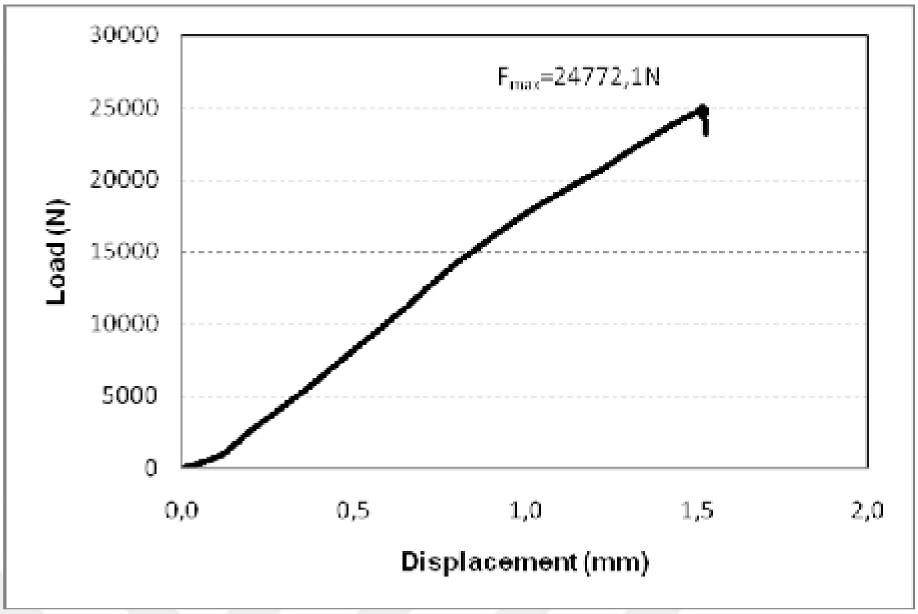

Figure 4.25. Typical load-displacement curve of composite sample during OHC test.

4.3. Numerical Method

4.3.1. Computer Aided Design (CAD)

Computer-aided design (CAD) is the process of creating a technical drawing with the use of computer software to facilitate assistance in the creation, modification, analysis, or optimization of a design. CAD software is used to increase the productivity of the designer, improve the quality of design, improve communications through documentation, and to create a database for manufacturing (Narayan et al., 2008). CAD software is used in many fields, such as automotive, shipbuilding, and aerospace industries, industrial and architectural design, prosthetics, and many more.

Graphic interfaces are often used to help in the creation and manipulation of the geometrical objects. There are numerous Computer Aided Design (CAD) software packages used for engineering design which can produce files containing the geometry of the designed engineering system. These files can usually be read in by modeling software packages, which can significantly save time when creating the geometry of the models. However, in many cases, complex objects read directly from a CAD file may need to be modified and/or simplified before performing meshing or discretization. It may be worth mentioning that there are CAD packages which incorporate modeling and simulation packages, and these are useful for the rapid prototyping of new products (Liu and Quek, 2003).

CATIA (Computer Aided Three-dimensional Interactive Application) is a multi-platform CAD/CAM/CAE commercial software suite developed by the French company Dassault Systèmes. Written in the C++ programming language, CATIA is the cornerstone of the Dassault Systèmes software suite. CATIA started as internal company use in 1977 by French aircraft manufacturer to develop Dassault's Mirage fighter jet and then was adopted in the aerospace, automotive, shipbuilding, and other industries (Anonymous, 2015g).

SolidWorks is a solid modeling computer-aided design software program that runs on Microsoft Windows. SolidWorks was founded in 1993 by Jon Hirschtick and produced by the Dassault Systèmes. SolidWorks application was first released in 1995 (Anonymous, 2015h).

4.3.2. Finite Element Method (FEM)

The finite element method (FEM) such as finite element analysis (FEA) is a numerical computational technique used to obtain approximate solutions of boundary value problems in engineering, stress distribution and deformation etc. occurred under forces in a structure can be calculated by using finite element method. In addition, analysis of heat transfer, dynamic, vibration and many others can be performed.

Structure analysis performed by generating a mesh by dividing into a certain number of elements in FEM. These elements are connected at points called nodes as shown in Figure 4.26 (Cook, 1995). Each element is connected to others at points called as a node. It can be selected to the different element types according to the analysis type and geometry of structure investigated. The stress, displacement, temperature information obtained in the analysis results that belongs to the node points. Taking average of these information in the node points, the information for the element is obtained.

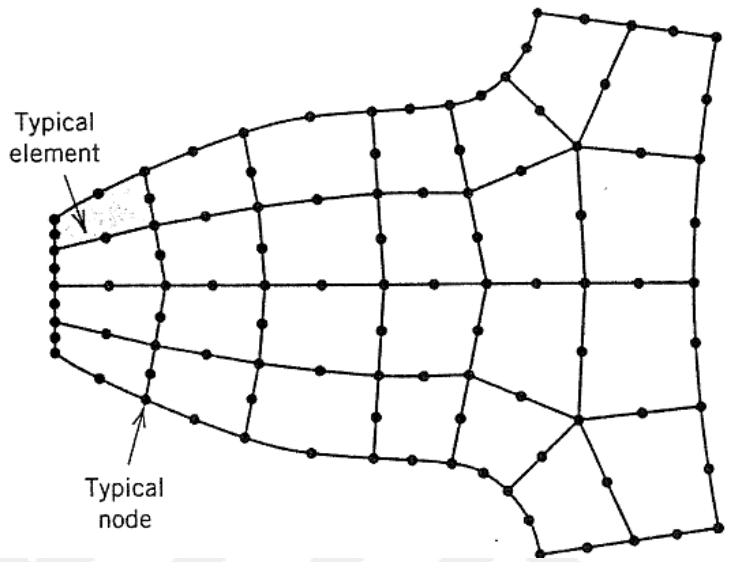

Figure 4.26. All nodes and elements lie in the plane of paper.

FEA has advantages over other numerical analysis methods.

- FEA is applicable to any field problem: heat transfer, stress analysis, magnetic fields, and so on.
- There is no geometric restriction. The body or region analyzed can have any shape.
- Boundary conditions and loading are not restricted. In stress analysis, any section of a body may be supported, while distributed or concentrated forces may be applied to any other section.
- Material properties are not restricted to isotropy and may change from one element to another.
- Components that have different behaviors and different mathematical descriptions can be combined.

5. PARAMETERS

5.1. Selected Chassis Type

The chassis is made up of a mixture of the monocoque and the platform frame types. Lower chassis type is a platform structure whereas upper chassis is a monocoque structure. It is modeled in Solid Works software program. Platform chassis frame is designed aluminum material and monocoque chassis is designed using carbon fiber-epoxy composite material. The dimensions of the platform chassis are 3740 mm in length, 1300 mm in width and chassis weighs about 160,89 kg, as shown in Figure 5.1. The dimensions of the monocoque chassis are 2611 mm in length, 1400 mm in width, 1200 mm in height and it weighs about 45 kg, as shown in Figure 5.2.

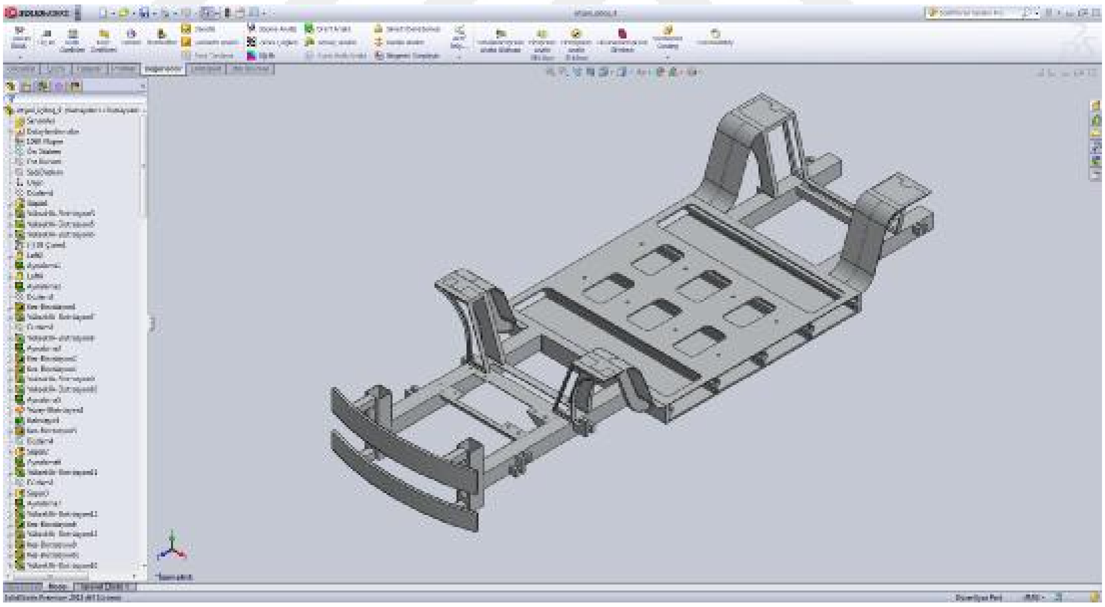

Figure 5.1. General view of the aluminum platform chassis in SolidWorks software.

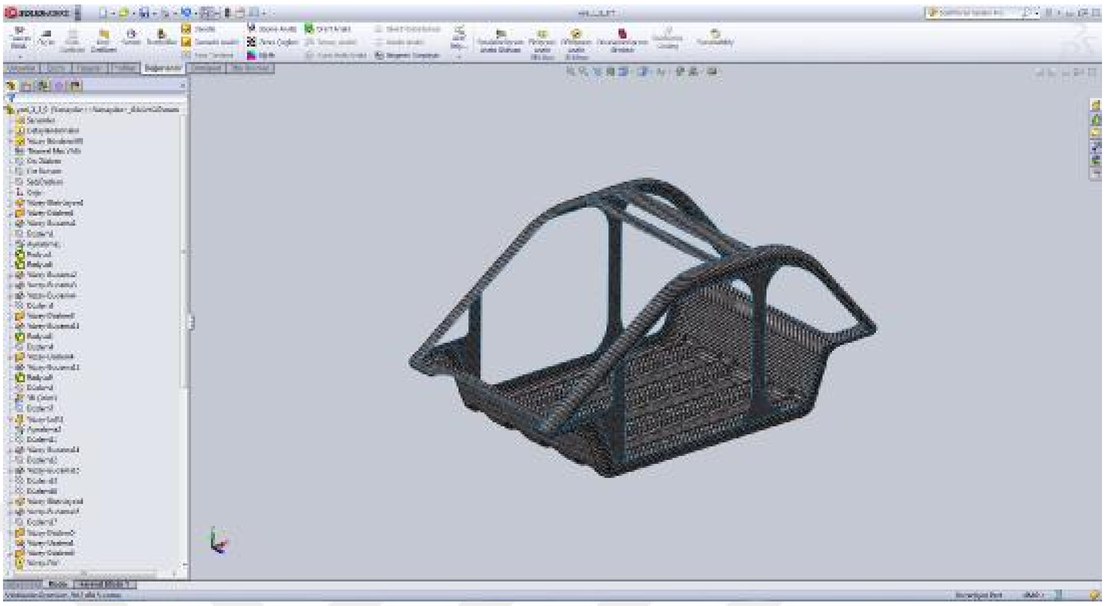

Figure 5.2. General view of the monocoque composite chassis in SolidWorks software.

5.2. Physical Properties of The Electric Vehicle Model

This vehicle is designed with two seater, DC motor, gearbox and battery groups. The range of an electric vehicle depends on the number and type batteries used. The weight of battery groups is 400 kg. So, it has average 169 km range value. The dimensions of electric vehicle are 3740 mm in length, 1300 mm in width, 1320 mm in height. Also wheelbase of electric vehicle is 2646,5 mm. Changing of batteries is possible with sliding drawers. Use of environmentalist and light motor characteristic and monocoque chassis made up of carbon fiber - epoxy composite material and platform chassis made up of aluminum alloy are the main reason to preferring for the cars of the future. Chassis weight of the designed vehicle is about 160.89 kg for the platform structure and 45 kg for the monocoque structure.

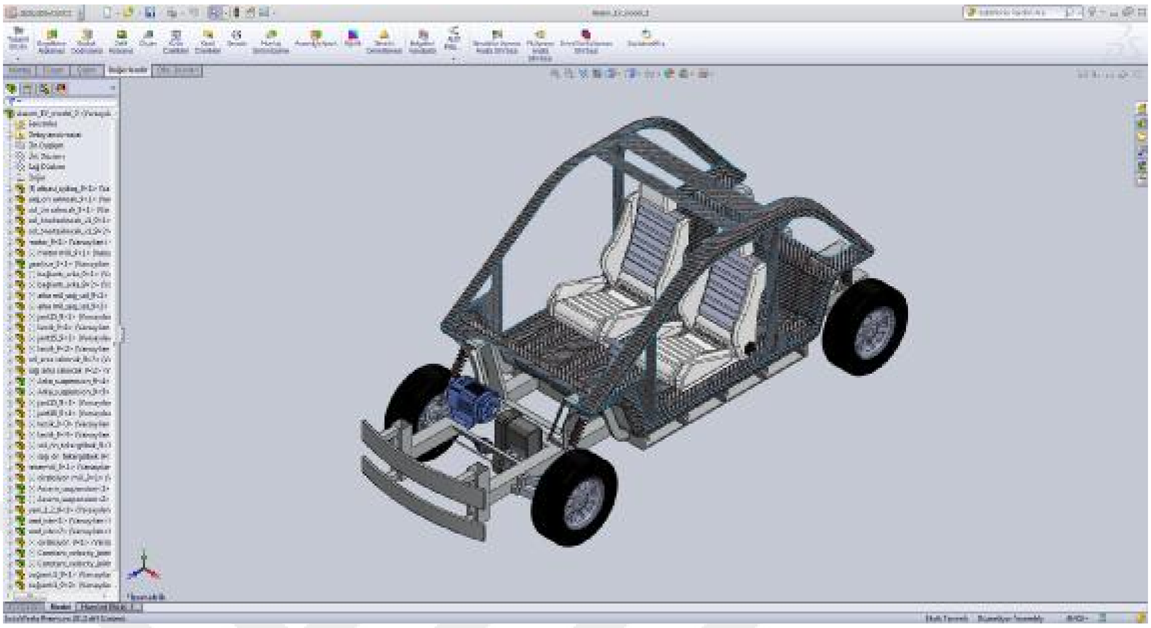

Figure 5.3. General view of Electric Vehicle model in SolidWorks software.

The specifications of the electric motor that is used in the study are as listed below;

Table.5.1. Technical specifications of electric motor

Model	M102 Motor
Type	DC Motor
Max Power	18.3 kW @ 1938.4 rpm
Max Torque	90.25 Nm @ 1938.4 rpm
Voltage	72 V
Max Efficiency	90%
Weight	86.18 kg
Motor Diameter	254 mm

Figure 5.4. M102 DC Motor

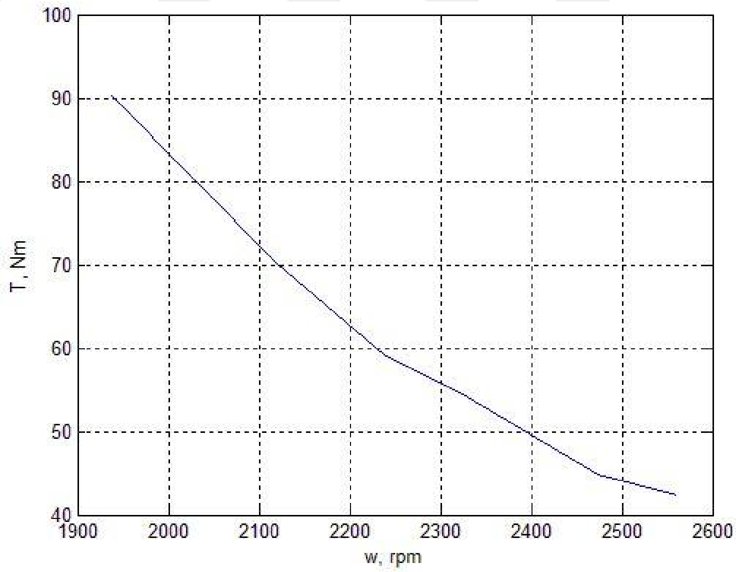

Figure 5.5. Torque - speed graph of the DC motor

The specifications of the battery that is used in the study are as listed below;

Table 5.2. Technical specifications of battery

Brand	Yuasa Dry Battery
Model	Yuasa NP12-12 Dry Battery
Voltage	12 V
Capacity	12 Ah
Dimensions	150x97x97 mm
Weight	4 kg

Figure 5.6. Yuasa 12V 12Ah Dry Battery

The specifications of the gearbox that is used in the study are as listed below;

Table 5.3. Technical specifications of the gearbox

Brand	Borg Warner
Model	31-03 eGeardrive
Speeds	Single
Available reduction ratios	6.54,7.17,8.00,8.28,8.76,9.07
Efficiency	97%
Rated input torque	200 Nm
Max input speed	14000 rpm
Center distance	210 mm
Lubrication	Splash
Weight	28 kg

Figure 5.7. Gearbox

Comparing with conventional IC vehicle, despite the heavy battery groups, the lightweight chassis structure is heavier than that of a IC engine based vehicle weight.

5.3. Mechanical Properties

As mentioned previously, in this study, carbon fiber reinforced-epoxy laminated composite material is used. The mechanical properties of this composite material are measured using Shimadzu AGS-X with class 0.5 100kN loadcell Test Machine in Mechanical Testing and the Investigating Laboratory in Mechanical Engineering Department at Adana Science and Technology University. These mechanical properties are presented in Table 5.4.

Table.5.4. Mechanical properties of carbon fiber-epoxy laminated composite

Material Properties	Symbol	Units	Values
Density	ρ_C	g/cm^3	1,54
Fiber volume fraction	V_f	%	55
Longitudinal modulus	E_{11}	GPa	137
Transverse modulus	E_{22}	GPa	10
Axial Poisson's ratio	v_{12}	-	0,30
Transverse Poisson's ratio	v_{21}	-	0,022
Longitudinal tension strength	X_t	MPa	1192
Transverse tension strength	Y_t	MPa	21
Longitudinal flexural strength	S_f^L	MPa	576,507
Transverse flexural strength	S_f^T	MPa	39,821
Longitudinal flexural modulus	E_B^L	GPa	95,319
Transverse flexural modulus	E_B^T	GPa	6,539
Longitudinal compression strength	X_c	MPa	305,28
Transverse compression strength	Y_c	MPa	64,7
Longitudinal compression modulus	E_{11}^C	MPa	-
Transverse compression modulus	E_{22}^C	MPa	-
Shear strength	S_{12}	MPa	59,45
Shear modulus	G_{12}	MPa	4705
Open hole compressive strength	F^{ohcu}	MPa	147

The material used to build this lower frame is Aluminum Alloy, its properties are shown in the Table 5.5.

Table 5.5. Mechanical properties of aluminum alloy

Density	2770 kg/m^3
Yield Strength	280 MPa
Modulus of Elasticity	71 GPa
Poisson's Ratio	0,33

5.4. Finite Element Analyses and Applied Loads

FEA of chassis is calculated in Ansys Workbench by using a CAD representation of the physical model. CAD representation of the chassis is cut into small elements. Meshed model has 656277 solid elements and 3452515 nodes. Meshed platform chassis is illustrated in Figure 5.8.

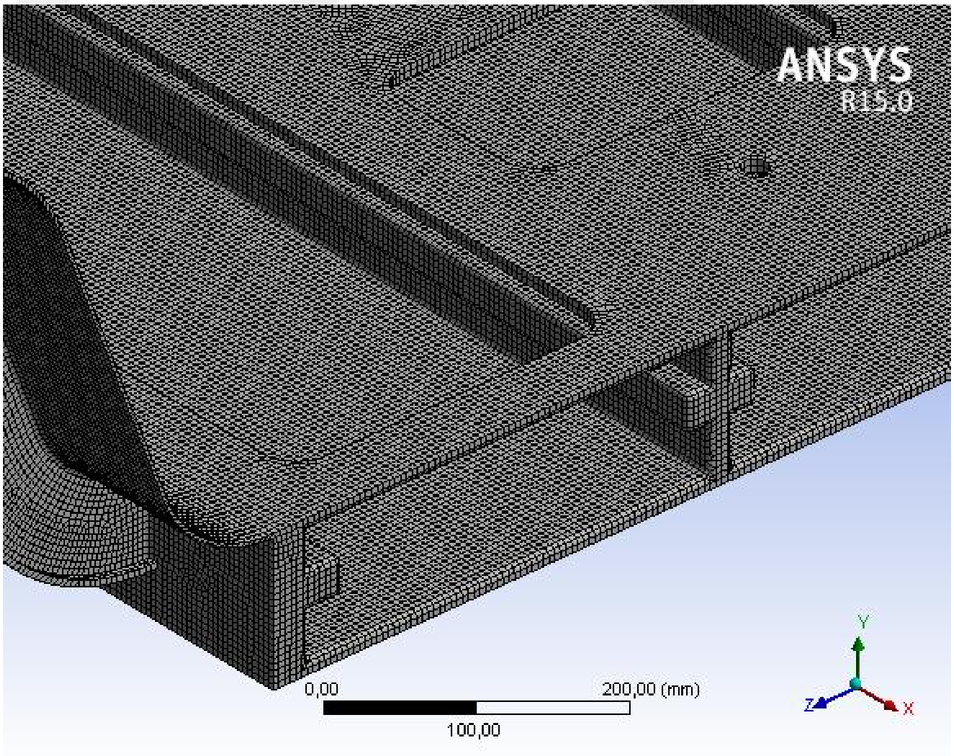

Figure 5.8. Meshed platform chassis

The weight of the driver, the passenger, electric motor, gearbox, battery groups etc. and impact of gravity are considered in the chassis analysis. These loads are applied statically at mounting points over the chassis. The front and the rear end of the chassis are fixed from wishbone and suspension arms at mounting points against rotation and translational. The loads used in the analysis are presented in Table 5.6.

Table 5.6. Applied loads on the chassis

Load on the chassis	Weight (kg)
DC Motor	86,18
Gearbox	28
Driver and Passenger	2x80
Battery Groups	400

4 different forces and 4 supported regions are applied on the chassis (Figure 5.9). Boundary conditions of the chassis are presented in Table 5.7.

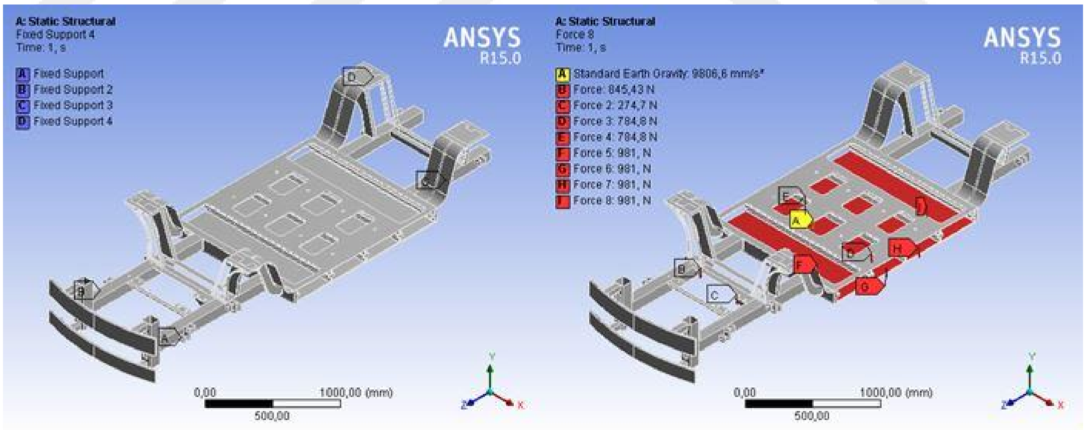

Figure 5.9. Forces and support regions

Table 5.7. Boundary conditions of the chassis

Symbol	Type of the Boundary Conditions	Representation	Magnitude
A	Standard Earth Gravity	Own weight of the chassis due to earth gravity	9806,6 mm/s^2
B	Fixed Support	Wishbone and suspension	-
C	Fixed Support	Wishbone and suspension	-
D	Fixed Support	Wishbone and suspension	-
E	Fixed Support	Wishbone and suspension	-
F	Force	Weight of DC motor	845,43 N
G	Force	Weight of gearbox	274,7 N
H	Force	Weight of driver	784,8 N
I	Force	Weight of passenger	784,8 N
J	Force	Weight of battery groups	981 N
K	Force	Weight of battery groups	981 N
L	Force	Weight of battery groups	981 N
M	Force	Weight of battery groups	981 N

The material used in building this lower frame is Aluminum Alloy, its properties are listed in Table 5.5. The material is defined by choosing it from Ansys material library. The material of this upper frame is carbon fiber-epoxy composite material, its properties is shown in the Table 5.4. It is added by defining its properties in Ansys library.

Integrated chassis which consisting of monocoque and platform structures have been analyzed in Ansys. Meshed model has 737885 solid elements and 2296632 nodes. Meshed chassis is illustrated in Figure 5.10.

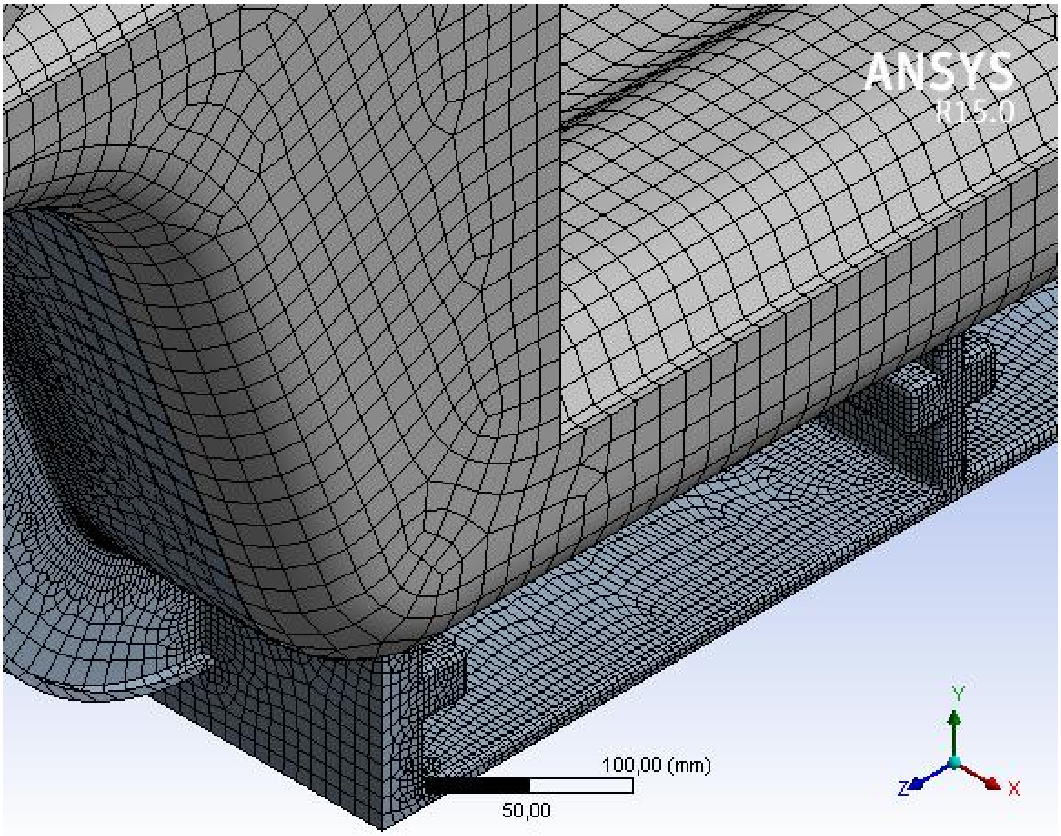

Figure 5.10. Meshed chassis

The weight of the driver, the passenger, electric motor, gearbox, battery groups etc. and gravity effect are considered in the chassis analysis. These loads are applied statically to mounting points over the chassis. The front and the rear end of the chassis are fixed from wishbone and suspension arms mounting points against rotational and translational motions.

4 different forces and 4 supported regions are applied on the chassis (Figure 5.11). Boundary conditions of the chassis are presented in Table 5.8.

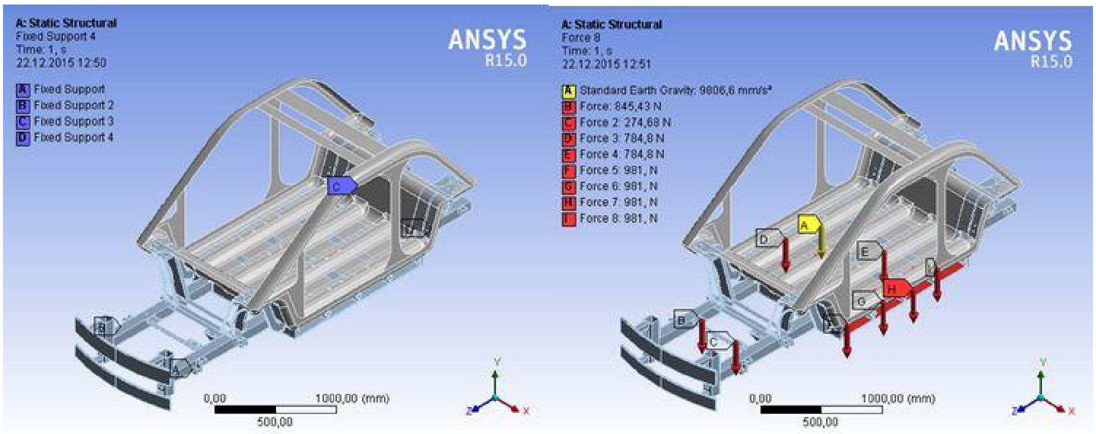

Figure 5.11. Forces and support regions

Table 5.8. Boundary conditions of the chassis

Symbol	Type of the Boundary Conditions	Representation	Magnitude
A	Standard Earth Gravity	Own weight of the chassis due to earth gravity	9806,6 mm/s^2
B	Fixed Support	Wishbone and suspension	-
C	Fixed Support	Wishbone and suspension	-
D	Fixed Support	Wishbone and suspension	-
E	Fixed Support	Wishbone and suspension	-
F	Force	Weight of DC motor	845,43 N
G	Force	Weight of gearbox	274,7 N
H	Force	Weight of driver	784,8 N
I	Force	Weight of passenger	784,8 N
J	Force	Weight of battery groups	981 N
K	Force	Weight of battery groups	981 N
L	Force	Weight of battery groups	981 N
M	Force	Weight of battery groups	981 N

The material used to build this lower frame is Aluminum Alloy, properties which are shown in the Table 5.5. the material is defined in Ansys by choosing it from Ansys material library. The material of this upper frame is carbon fiber-epoxy composite, and its properties are shown in the Table 5.4. It is added to the analysis by defining related properties in Ansys library.

6. RESULTS AND DISCUSSION

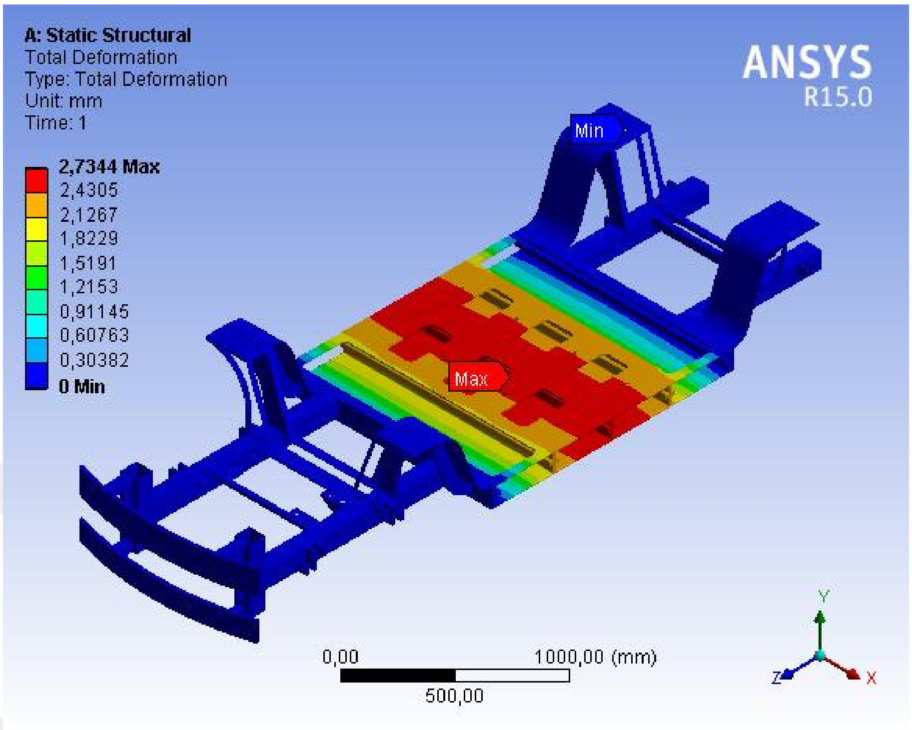

Figure 6.1. Total deformation of the chassis

Maximum deflection was observed in the center of driver cabin floor and noted down its position to strengthen it. Maximum deformation point with 2.7344 mm is shown in Figure 6.1.

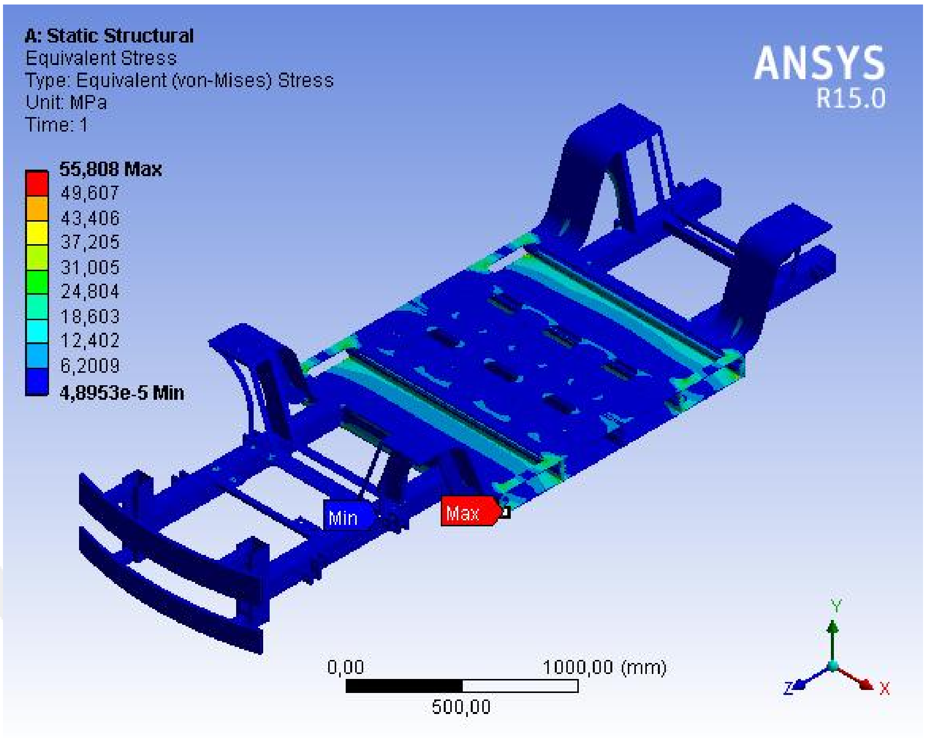

Figure 6.2. von-Mises stress of the chassis

Results showed that maximum von-Mises stress of the design is 55.808 MPa and the value is far below the material's yield strength of 280 MPa and also maximum Von-Mises stress point as shown in Figure 6.2. Most of the areas throughout chassis were observed to be subjected to minimum value of stress as shown in stress distribution tree in Figure 6.2.

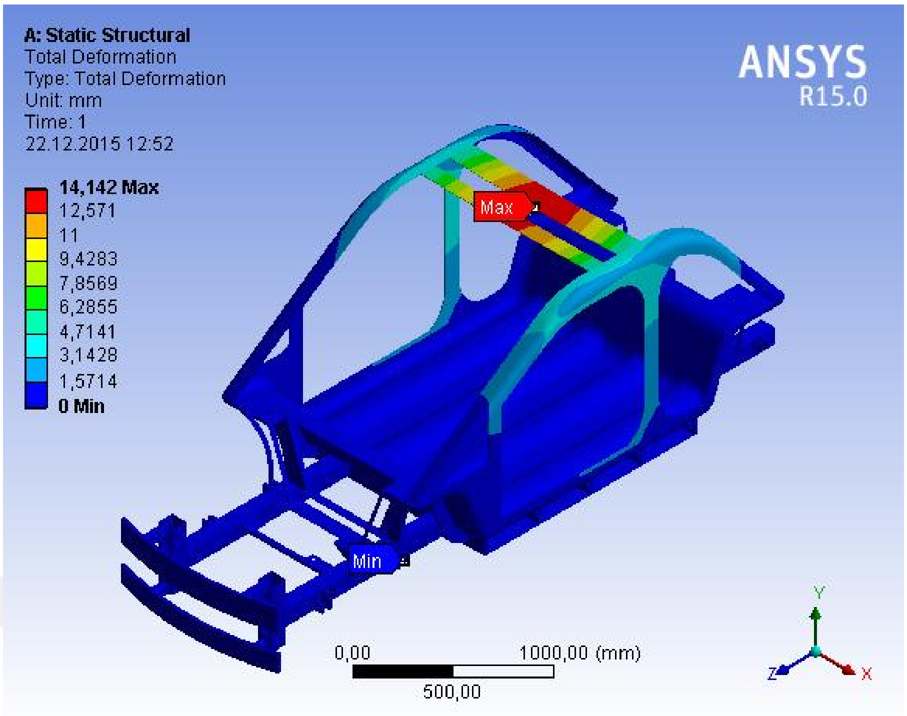

Figure 6.3. Total deformation of the chassis

Maximum deflection was observed in the top of the vehicle cabin and noted down its position to strengthen it. Maximum deformation point with 14,142 mm is shown in Figure 6.3.

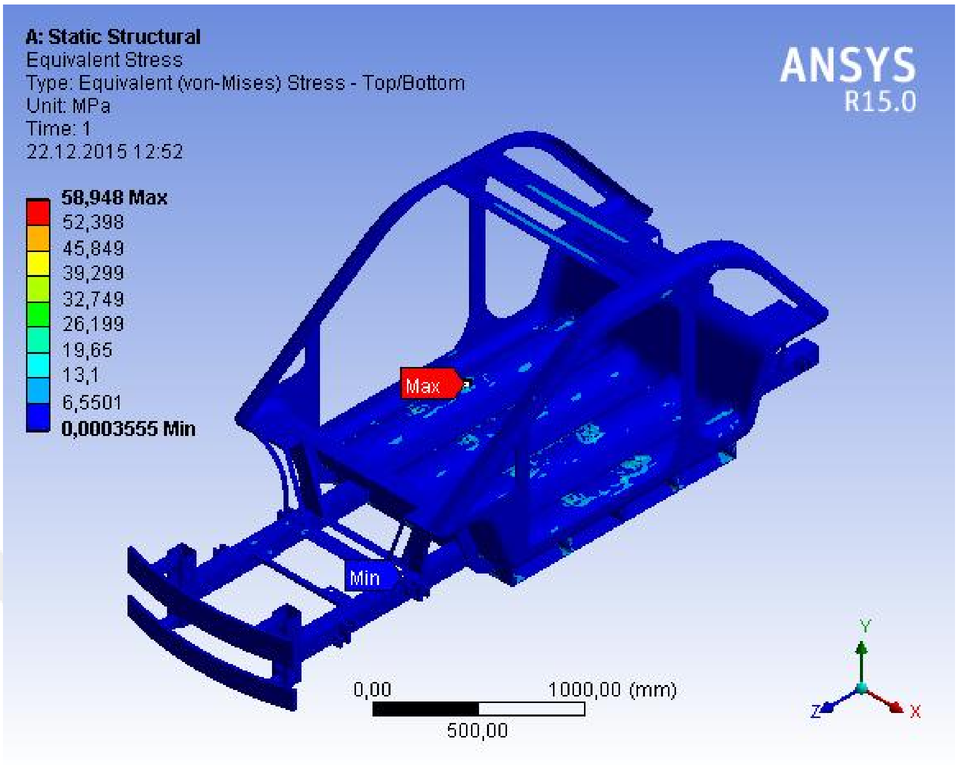

Figure 6.4. von-Mises stress of the chassis

Results showed that maximum von-Mises stress of the design is 58.948 MPa and also maximum Von-Mises stress point as shown in Figure 6.4. Most of the areas throughout chassis were observed to be subjected to minimum value of stress as shown in stress distribution tree in Figure 6.4.

In this thesis, the strength of composite chassis is investigated against static forces. Platform and monocoque chassis are handled separately in the analyses of the Ansys software program. In this analysis, only total deformation of Aluminum chassis is 2,7344 mm and Von - misses stress value of aluminum chassis is 55,808 MPa. If we evaluate separately, with connect of two different chassis total deformation and Von-Misses stress values are 14,142 mm and 58,948 MPa. As can be seen from the results, the assembly of two elements of the chassis leads to better results. This simply increases the strength of chassis. Actually, main issue to be considered is the joining method for these two chassis. For example, in this thesis, looking at the analysis results, the connection of the two chassis elements are defined by bonded contact by Ansys software program. On the other hand, if preferred, assembly can be achieved by bolt and nuts, with frictionless methods. This may vary the results of analysis and make it more realistic.

While use of only carbon fiber - epoxy composite for the chassis manufacture has an advantage about weight of vehicle, this configuration is not be strong enough against external forces. For that reason, carbon fiber - epoxy chassis must be support with aluminum to protect the lightweight of chassis.

7. CONCLUSION

The aim of study was design and development of a light weight chassis for an electric vehicle. Firstly, previous studies and similar works were examined. Secondly, the carbon fiber - epoxy composite laminated material was manufactured and many tests are performed to determine mechanical properties of composite material. Thirdly, design of chassis is made by use of SolidWorks software program. FEA analysis of chassis is obtained in the Ansys using the experimental data . According to this result, some improvements are achieved with the developed chassis. The chassis is supported with an aluminum platform. Final analyses proved that the developed chassis is a very successful one.

The use of aluminum platform chassis undertook some specific loads particularly weight of driver, passenger, DC motor, gearbox and battery groups. So, it reduced the forces over the monocoque composite chassis. Having obtaining the results for the presented chassis, it has been shown that it withstands the applied forces.

In future, different chassis types for electric vehicle can be developed. The chassis configurations for specific purposes can also be manufactured. However, it is clear that the composite chassis designs are far from withstanding the loads in IC engine based or electric cars due to engine and battery loads, respectively. Therefore, unless heavy IC engine or heavy battery weight problems for electric cars are solved, there is a need for light weight support of the composite chassis used.

REFERENCES

AGRAWAL, M. S., & RAZIK, M., 2013. Finite Element Analysis of Truck Chassis. International Journal of Engineering Sciences & Research Technology , 2 (12), 3432-3438.

AKBAŞ, H., GÜÇ, F., US, S., & KUNTAY, A., 2006. Treyler Şasisi Yapısal Dayanıklılık ve Ömür Analizi. Kongresi, Otomotiv Teknolojileri. Bursa.

ANONYMOUS, 2015a. https://en.wikipedia.org/wiki/Lagonda (Access Date: 13 September 2015).

ANONYMOUS, 2015b. https://en.wikipedia.org/wiki/Backbone_chassis (Access Date: 13 September 2015).

ANONYMOUS, 2015c. https://en.wikipedia.org/wiki/Monocoque (Access date: 24.08.2015) .

ANONYMOUS, 2015d. http://www.lotuscars.com/chassis-evora (Access Date: 13 September 2015).

ANONYMOUS,2015e.https://en.wikipedia.org/wiki/Citro%C3%ABn_Traction_Avant (Access Date: 13 September 2015).

ANONYMOUS, 2015f. http://www.worldautosteel.org/projects/ulsab/ulsab-image-gallery/ (Access Date: 13 September 2015).

ANONYMOUS, 2015g. https://en.wikipedia.org/wiki/CATIA (Access Date: 30 October 2015).

ANONYMOUS, 2015h. https://en.wikipedia.org/wiki/SolidWorks (Access Date: 30 October 2015).

ANONYMOUS, 2015ı. https://en.wikipedia.org/wiki/BMW_i3 (Access Date: 28 October 2015).

ANONYMOUS, 2015i. https://en.wikipedia.org/wiki/BMW_i8 (Access Date: 28 October 2015).

ANONYMOUS, 2015j. http://www.lexus-int.com/models/LFA/wonder-material.html (Access Date: 28 October 2015).

ANONYMOUS, 2015k. http://www.fiat500usa.com/2013/09/alfa-romeo-4c-overview.html (Access Date: 28 October 2015).

ASTM Standards and Literature References for Composite Materials, (2000).Standard Test Methods for Density and Specific Gravity (Relative Density) of Plastics by Displacement D792-00.American Society for Testing and Material, Philadelphia, PA.

ASTM Standards and Literature References for Composite Materials, (2000).Standard Test Method for Ignition Loss of Cured Reinforced Resins D2584-02.American Society for Testing and Material, Philadelphia, PA.

ASTM Standards and Literature References for Composite Materials, (2000).Standard Test Method for Tensile Properties of Polymer Matrix Composite Plates D3039M-00.American Society for Testing and Material, Philadelphia, PA.

ASTM Standards and Literature References for Composite Materials, (2002).Standard Test Methods for Flexural Properties of Unreinforced and Reinforced Plastics and Electrical Insulating Materials D790-02.American Society for Testing and Material, Philadelphia, PA.

ASTM Standards and Literature References for Composite Materials, (2003).Standard Test Method for Compressive Properties of Polymer Matrix Composite Materials with Unsupported Gage Section by Shear Loading D3410M-03.American Society for Testing and Material, Philadelphia, PA.

ASTM Standards and Literature References for Composite Materials, (1998).Standard Test Method for Shear Properties of Composite Materials by the V-Notched Beam Method D5379M-98.American Society for Testing and Material, Philadelphia, PA.

ASTM Standards and Literature References for Composite Materials, (2004).Standard Test Method for Open-Hole Compressive Strength of Polymer Matrix Composite Laminates D6484M-04.American Society for Testing and Material, Philadelphia, PA.

BADIE, M. A, MAHDI, E, HAMOUDA, A. M. S., 2011. An Investigation into Hybrid Carbon/Glass Fiber Reinforced Epoxy Composite Automotive Drive Shaft. Materials and Design , 32, 1485–1500.

BAJWA, M. S., RATURI, Y., & JOSHI, A., 2013. Static Load Analysis of Tata Super Ace Chassis and Its Verification Using Solid Mechanics. International Journal of Mechanical and Production Engineering , 1 (2), 55-58.

BARTUS, S. D., VAIDYA, U. K., & ULVEN, C. A., 2006. Design and Development of a Long Fiber Thermoplastic Bus Seat . Journal of Thermoplastic Composite Materials , 19, 131-154.

BHASKAR, E., MUNEIAH, T., RAJESH, C.V., 2014. Static and Dynamic Analysis of Chassis. International Journal of Research, 1 (6), 320-328.

BROWN J. C., ROBERTSON A. J., SERPENTO S. T., 2002b. Motor Vehicle Structures: Concepts and Fundamentals, 1st Edition, Butterworth - Heinemann, Oxford, 302p.

BROWN J. C., ROBERTSON A. J., SERPENTO S. T., 2002. Terminology and Overview of Vehicle Structure Types (D. A. CROLLA editor). Automotive Engineering Powertrain, Chassis System and Vehicle Body, 1st Edition, Butterworth - Heinemann, Oxford, pp. 527 - 541.

CARPENTER, J. A., 2008. Challenges and opportunities for automotive composites, SPE Automotive Composites Conference and Exposition, Troy, MI, USA, CD Rom Proceedings.

COOK, R. D., 1995 “Finite Element Modeling for Stress Analysis”, John Wiley &Sons Ltd., New York, 1-144.

CRAMER, D. R., & TAGGART, D. F., 2002. Design and Manufacture of an Affordable Advanced-Composite Automotive Body Structure. The 19th International Battery, Hybrid and Fuel Cell Electric Vehicle Symposium & Exhibition, (pp. 1-12). Busan.

CROCCOLO, D., AGOSTINIS, M. D., & VINCENZI, N., 2011. Structural Analysis of an Articulated Urban Bus Chassis via FEM: a Methodology Applied to a Case Study. Journal of Mechanical Engineering , 11 (57), 799-809.

FERABOLI, P., & MASINI, A., 2004. Development of Carbon/Epoxy Structural Components for a High Performance Vehicle. Composites: Part B , 35, 323-330.

FERABOLI, P., MASINI, A., TARABORRELLI, L., & PIVETTI, A., 2007. Integrated Development of CFRP Structures for a Topless High Performance Vehicle. Composite Structures , 78, 495-506.

FRANCIS, V., RAI, R. K., SINGH, A. K., SINGH, P. K., & YADAV, H., 2014. Structural Analysis of Ladder Chassis Frame for Jeep Using Ansys. International Journal of Modern Engineering Research , 4 (4), 41-47.

GIBSON, R.F., 1994. Principals of Composite Material Mechanics. McGraw-Hill.

GODSE, S., & PATEL, D. A., 2013. Static Load Analysis of Tata Ace Ex Chassis and Stress Optimisation Using Reinforcement Technique. International Journal of Engineering Trends and Technology , 4 (7), 3037-3039.

JACOB, A., 2010. BMW Counts on Carbon Fiber for its Megacity Vehicle. Journal of Reinforced Plastic Composite , 54, 38-41.

JEON, S. H., KIM, H. M., PARK, T. H., CHOI, B. H., & CHOI, W. C., 2011. Development os Polycarbonate/Acrylonitrile-Butadiene-Styrene Copolymer Based Composites with Functional Fillers for Car Audio Chassis. Materials and Design , 32, 1306-1314.

JONES, R. M., 1998. Mechanics of Composite Materials (2th ed.). US: Taylor &Francis Inc.

KIM, D. H., KIM, H. G., KIM, H. S., 2015. Design Optimization and Manufacture of Hybrid Glass/Carbon Fiber Reinforced Composite Bumper Beam for Automobile Vehicle. Composite Structures , 131, 742-752.

KUMAR, P., MURALIDHARAN, V., & MADHUSUDHANA, G., 2014. Design and Analysis of a Tubular Space Frame Chassis of a High Performance Race Car. International Journal of Research in Engineering and Technology , 3 (2), 497-501.

LAVANYA, D., MAHESH, G. G., AJAY, V., & YUVARAJ, C., 2014. Design and Analysis of a Single Seater Race Car Chassis Frame. International Journal of Research in Aeronautical and Mechanical Engineering , 2 (8), 12-23.

LEE, D. G., KIM, H. S., KIM, J. W., & KIM, J. K., 2004. Design and Manufacture of an Automotive Hybrid Aluminum/Composite Drive Shaft. Composite Structures , 63, 87-99.

LI, Y., LIN, Z., JIANG, A., & CHEN, G., 2004. Experimental Study of Glass-Fiber Mat Thermoplastic Material Impact Properties and Lightweight Automobile Body Analysis. Materials and Design , 25, 579-585.

LIU, Q., LIN, Y., ZONG, Z., SUN, G., & LI, Q., 2013. Lightweight Design of Carbon Twill Weave Fabric Composite Body Structure for Electric Vehicle. Composite Structures , 97, 231-238.

LIU, G. R. and QUEK, S. S., 2003. Computational Modelling (G. R. LIU and S. S. QUEK, edts). Finite Element Method: A Practical Course, ButterworthHeinemanni, Oxford, UK, pp. 1-11.

MALLICK, P. K., 1993. Fiber-reinforced composites materials, manufacturing, and design, (2 nded.). New York: Marcel Decker.

MAT, M. H., & GHANI, A. R., 2012. Design and Analysis of 'Eco' Car Chassis. Procedia Engineering (41), 1756-1760.

MCAULEY, J. W.,2003. Global Sustainability and Key Needs in Future Automotive Design. Environ Sci Technol , 37:5414–6.

NARAYAN, K. L., RAO, K. M. and SARCAR, M. M. M., 2008. Computer Aided Design and Manufacturing. New Delhi: Prentice Hall of India. p.3.

NING, H., JANOWSKI, G. M., VAIDYA, U. K., & HUSMAN, G., 2007a. Thermoplastic Sandwich Structure Design and Manufacturing for the Body Panel of Mass Transit Vehicle. Composite Structures , 80, 82-91.

NING, H., PILLAY, S., & VAIDYA, U. K., 2009. Design and Development of Thermoplastic Composite Roof Door for Mass Transit Bus . *Materials and Desgn , 30*, 983-991.

NING, H., VAIDYA, U., JANOWSKI, G. M., & HUSMAN, G., 2007b. Design, Manufacture and Analysis of a Thermoplastic Composite Frame Structure for Mass Transit. *Composite Structures , 80*, 105-116.

NOR, M. A., RASHID, H., MAHYUDDIN, W. M., AZLAN, M. A., & MAHMUD, J., 2012. Stress Analysis of a Low Loader Chassis. *Procedia engineering* (41), 995-1001.

OKUTAN, B., 2001. Stress and failure analysis of laminated composite pinned joints. PhD Thesis, Dokuz Eylül University, Izmir.

PARK, C. K., KAN, C. D., & HOLLOWELL, W. T., 2013. Evaluation of Crashworthiness of a Carbon Fibre Reinforced Polymer (CFRP) Ladder Frame in a Body on Frame Vehicle. International Journal of Crashworthiness , 19 (1), 27-41.

PATEL, H., PANCHAL, K. C., & JADAV, C. S., 2013. Structural Analysis of Truck Chassis Frame and Design Optimization for Weight Reduction. International Journal of Engineering and Advanced Technology , 2 (4), 665-668.

PATEL, R. L., GAWANDE, K. R., & MORABIYA, D. B., 2014. Design and Analysis of Chassis Frame of TATA 2516TC. International Journal for Research in Applied Science and Engineering Technology , 2 (3), 115-119.

PATEL, T. M., BHATT, M. G., & PATEL, H. K., 2013. Analysis and Validation of Eicher 11.10 Chassis Frame Using Ansys. International Journal of Emerging Trends & Technology in Computer Science , 2 (2), 85-88.

PATIL, H. B., & KACHAVE, S. D., 2013. Effects of Web and Flange Thickness on Bending Stiffness of Chassis. International Journal of Advance Research in Science and Engineering , 2 (7), 53-61.

PATIL, H. B., KACHAVE, S. D., & DEORE, E. R., 2013. Stress Analysis of Automotive Chassis with Various Thicknesses. Journal of Mechanical and Civil Engineering , 6 (1), 44-49.

RILEY, W. B. and GEORGE, A. R., 2002. Design, Analysis and Testing of a Formula SAE Car Chassis. SAE Motorsports Engineering Conference and Exhibition, 18p.

SAVAGE, G., 2010. Formula 1 Composites Engineering. Engineering Failure Analysis , 17, 92-115.

SINGH, A., SONI, V., & SINGH, A., 2014. Structural Analysis of Ladder Chassis for Higher Strength. International Journal of Emerging Technolgy and Advenced Engineering, 4 (2), 253-259.

SINGH, R. P., 2010. Structural Performance Analysis of Formula SAE Car. Journal Mekanikal (31), 46-61.

SOLGHAR, A. A., & ARSALANLOO, Z., 2013. The Stress Analysis of Minibus Chassis Using Finite Element Method. Caspian Journal of Applied Sciences Research , 2 (5), 20-25.

STAAB, G. H., 1999. Laminar Composites (1th ed.). US: Butterworth-Heinemann.

SWAMI, K. I., & TULJAPURE, S. B., 2014. Analysis of Ladder Chassis of Eicher 20.16 Using FEM. Journal of Applied Geology and Geophysics , 2 (1), 6-13.

TEBBY, S., ESMAILZADEH, E., BARARI, A., 2011. Methods to Determine Torsion Stiffness in an Automotive Chassis. Computer-Aided Design and Applications, 67-75.

THATTAIPARTHASARATHY, K. B., PILLAY, S., NING, H., & VAIDYA, U. K., 2008. Process Simulation, Design and Manufacturing of a Long Fiber Thermoplastic Composite for Mass Transit Application. Composites: Part A , 39, 1512-1521.

VAIDYA, U. K., SAMALOT, F., PILLAY, S., JANOWSKI, G. M., HUSMAN, G., & GLEICH, K., 2004. Design and Manufacture of Woven Reinforced Glass/Polypropylene Composites for Mass Transit Floor Structure. Journal of Composite Materials , 38 (21), 1949-1972.

VIJAYKUMAR, P., & PATEL, R. I., 2012. Structural Analysis of Automotive Chassis Frame and Design Modification for Weight Reduction. International Journal of Engineering Research & Technology , 1 (3), 1-6.

WALRATH, D. E. and ADAMS, D. F.,1983. The Iosipescu shear test as applied to composite materials, Exp. Mech., 23:105.

http://www.electriccarpartscompany.com, (Access Date: 18 December 2015).

https://www.borgwarner.com, (Access Date: 20 December 2015).

http://www.pilsitesi.com, (Access Date: 20 December 2015).

CURRICULUM VITAE

Himmet ÖZARSLAN was born in Adana on September 01, 1982. After completing his education in Öğretmen Zeynep Erdoğdu Primary Education and Ahmet Kurttepeli High School, he enrolled in Mustafa Kemal University Mechanical Engineering Department in 2001. He had graduated from the Mechanical Engineering Department of Mustafa Kemal University with a Bachelor of Science degree in 2006. He started his Master of Science education in Automotive Engineering Department of Çukurova University in 2013. He has been working as a Research Assistant in Çukurova University since 2013.